Cosmic Ray Composition and Spectra : Progress since Aspen 05

Gaurang B. Yodh
UC Irvine

In this talk I outline my take on the question of composition from about 1 TeV to the highest energies.

Important point I emphasize is to separate what has been measured and what has been interpreted and how the two are intertwined.

First I review direct measurments near the top of the atmosphere:
What is definite and what is not resolved:

Then I discuss the measurements in the energy range between about 10 TeV and 10 PeV :
EAS and ACT measurements
What is the status of current measurements on the composition ?
What are some of the problems to be resolved.

Finally I what are the problems in understanding the experimental results and model interpretations.

I start by showing a compilation of results by Horandel (2006) to indicate that the present state is complex to say the least.

Then I show recent results from the CREAM experiment and compare them to existing results from JACEE, RUNJOB and other balloon experiments.

After that I summarize the situation at higher energies where all our experiments are indirect.

The talk is meant to stimulate discussions and generate ideas as to how to improve the current unresolved state of affairs.

Bird's eye view of Spectra of Cosmic Rays

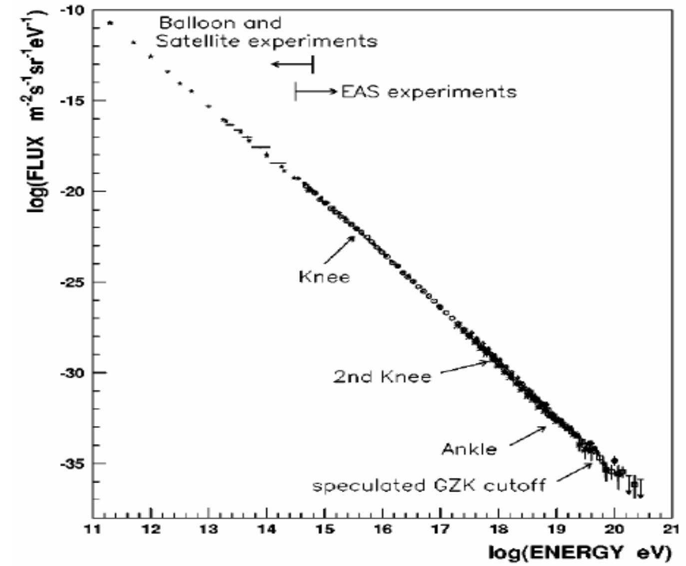

Composition of Cosmic Rays

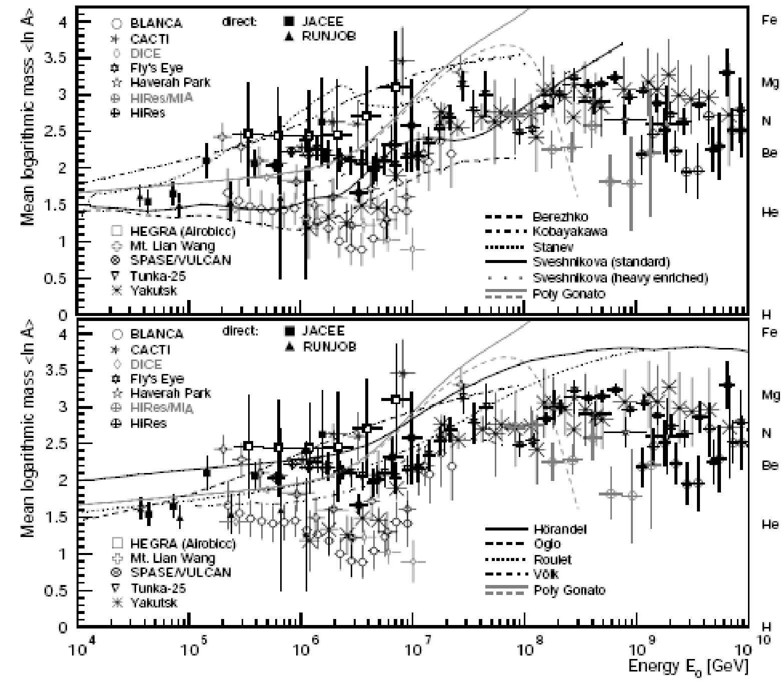

Fig. 12. Mean logarithmic mass of cosmic rays derived from the average depth of the shower maximum, see Fig. 10. As hadronic interaction model used to interpret the measurements serves a modified version of QGSJET 01 with lower cross sections and a slightly increased elasticity (model 3a (Hörandel, 2003b)). For experimental references, see caption of Fig. 10. For comparison, results from direct measurements are shown as well from the JACEE (JACEE collaboration, 1999) and RUNJOB (Derbina et al., 2005) experiments.
Models: The the grey solid and dashed lines indicate spectra according to the poly-gonato model (Hörandel, 2003a).
Top: The lines indicate spectra for models explaining the knee due to the maximum energy attained during the acceleration process according to Sveshnikova (2003) (—, · · · ·), Berezhko and Ksenofontov (1999) (- - -), Stanev et al. (1993) (· · ·), Kobayakawa et al. (2002) (-·-·).
Bottom: The lines indicate spectra for models explaining the knee as effect of leakage from the Galaxy during the propagation process according to Hörandel et al. (2007) (—), Ogio and Kakimoto (2003) (- - -), Roulet (2004) (· · ·), as well as Völk and Zirakashvili (2003) (-·-·).

Detailed view of spectra:

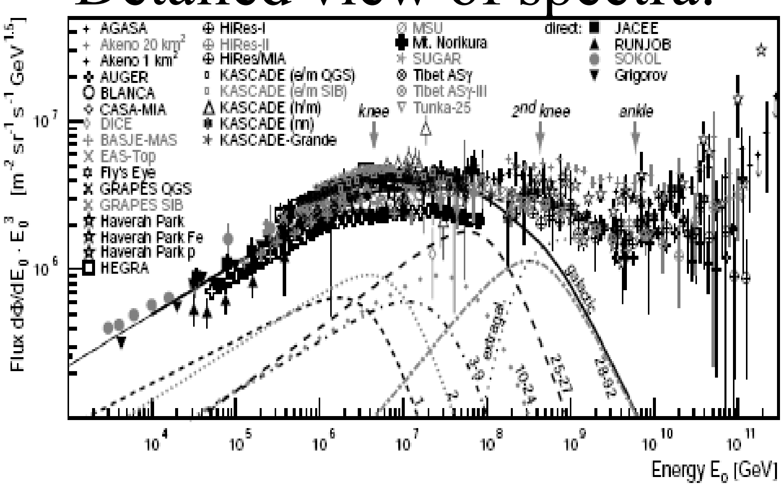

Fig. 8. All-particle energy spectrum of cosmic rays, the flux is multiplied by E^3. Results from direct measurements by Grigorov et al. (Grigorov et al., 1999), JACEE (Asakimori et al., 1998), RUNJOB (Derbina et al., 2005), and SOKOL (Ivanenko et al., 1993) as well as from the air shower experiments AGASA (Takeda et al., 2003), Akeno 1 km^2 (Nagano et al., 1984a), and 20 km^2 (Nagano et al., 1984b), AUGER (Sommers et al., 2005), BASJE-MAS (Ogio et al., 2004), BLANCA (Fowler et al., 2001), CASA-MIA (Glasmacher et al., 1999b), DICE (Swordy and Kieda, 2000), EAS-TOP (Aglietta et al., 1999), Fly's Eye (Corbato et al., 1994), GRAPES-3 interpreted with two hadronic interaction models (Hayashi et al., 2005), Haverah Park (Lawrence et al., 1991) and (Ave et al., 2003), HEGRA (Arqueros et al., 2000), HiRes-MIA (Abu-Zayyad et al., 2001a), HiRes-I (Abbasi et al., 2004), HiRes-II (Abbasi et al., 2005), KASCADE electrons and muons interpreted with two hadronic interaction models (Antoni et al., 2005), hadrons (Hörandel et al., 1999), and a neural network analysis combining different shower components (Antoni et al., 2002), KASCADE-Grande (preliminary) (Haungs et al., 2006b), MSU (Fomin et al., 1991), Mt. Norikura (Ito et al., 1997), SUGAR (Anchordoqui and Goldberg, 2004), Tibet ASγ (Amenomori et al., 2000a) and ASγ-III (Amenomori et al., 2003), Tunka-25 (Chernov et al., 2006), and Yakutsk (Glushkov et al., 2003). The lines represent spectra for elemental groups (with nuclear charge numbers Z as indicated) according to the poly-gonato model (Hörandel, 2003a). The sum of all elements (galactic) and a presumably extragalactic component are shown as well. The dashed line indicates the average all-particle flux at high energies.

Large scatter in ' measured ' quantities due to:
Systematics in energy determination and in shower simulations.

Horandel: astro-ph/0702370v1

I. Measurements above the atmosphere: CREAM

CREAM: COSMIC RAY ENERGETICS AND MASS

Cosmic Ray Energetics and Mass

Seo et al. Adv. in Space Res., **33** (10), *1777*, 2004.

- Complementary Charge Measurements
  - Timing-Based Charge Detector
  - Cherenkov Counter
  - Pixelated Silicon Charge Detector
  - Scintillating Fiber hodoscopes
- Complementary Energy Measurements
  - Transition Radiation Detector (velocity for $Z \geq 3$)
  - Tungsten-Scintillator Calorimeter (energy for $Z \geq 1$)
  - <u>In-flight cross-calibration</u> with $Z > 3$ particles in both detectors ensures best possible energy determination
- Large acceptance:
  - 2.2 m^2sr trigger aperture

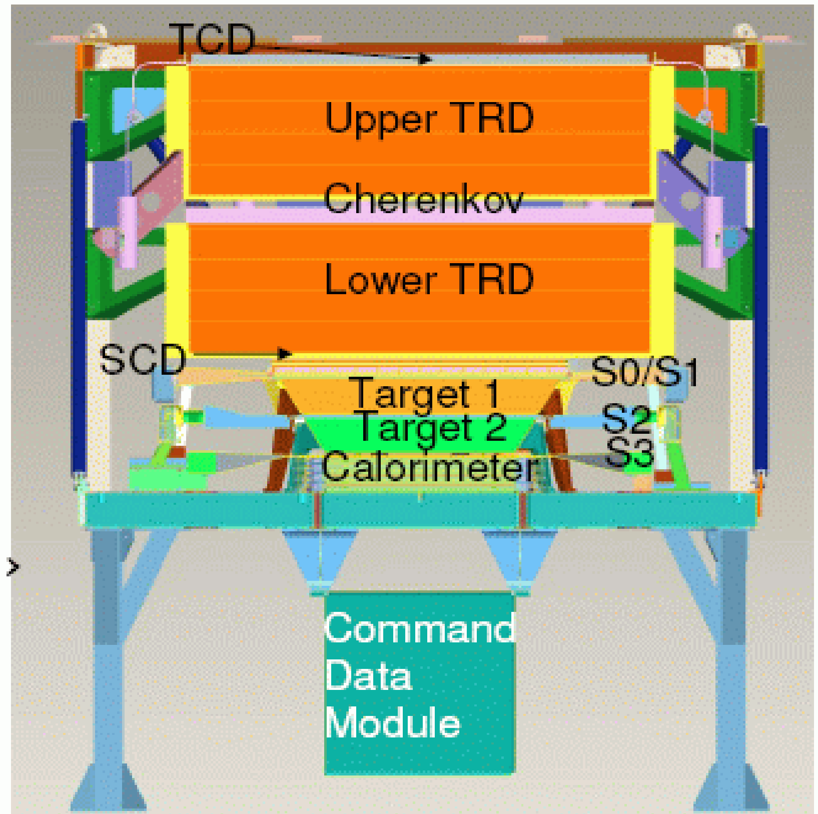

71 inch (~1.8 m)

Modular Design for Recovery

Monte Carlo Simulations

H.S. Ahn et al., Proc. 27th ICRC (Hamburg), 6, 2159, 2001

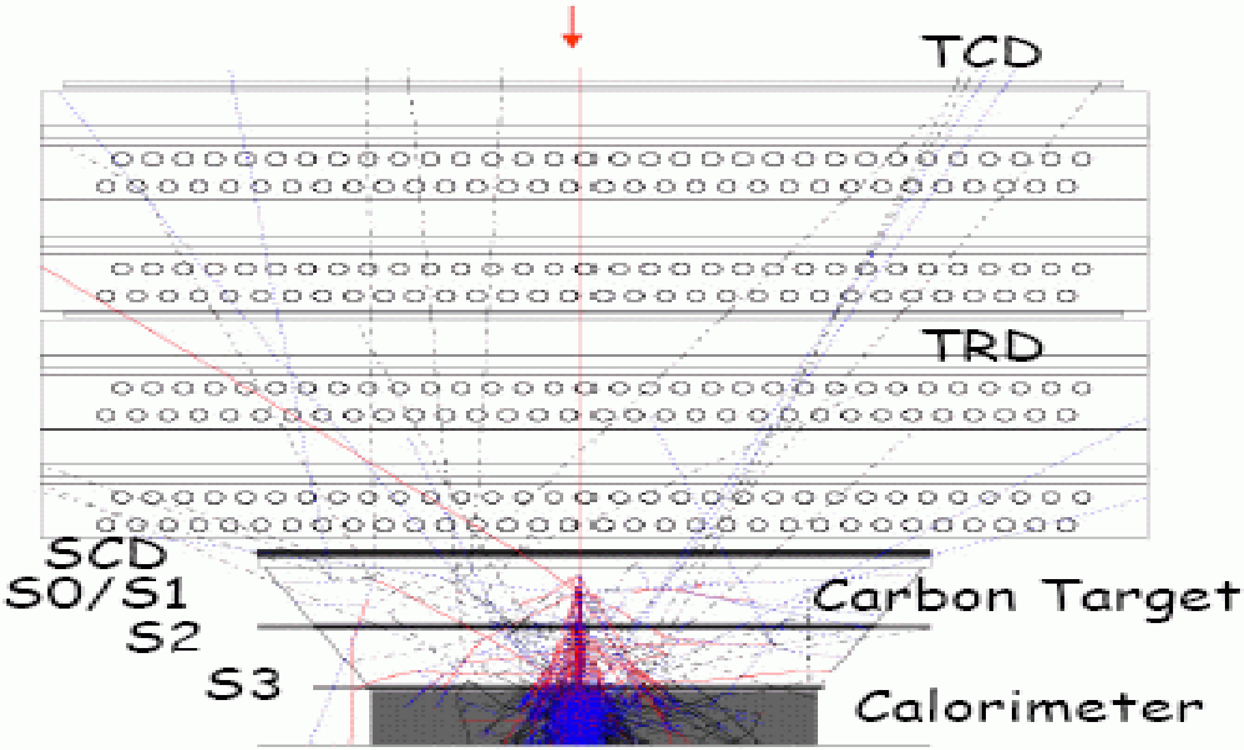

CREAM III: Instrument assembly at Maryland

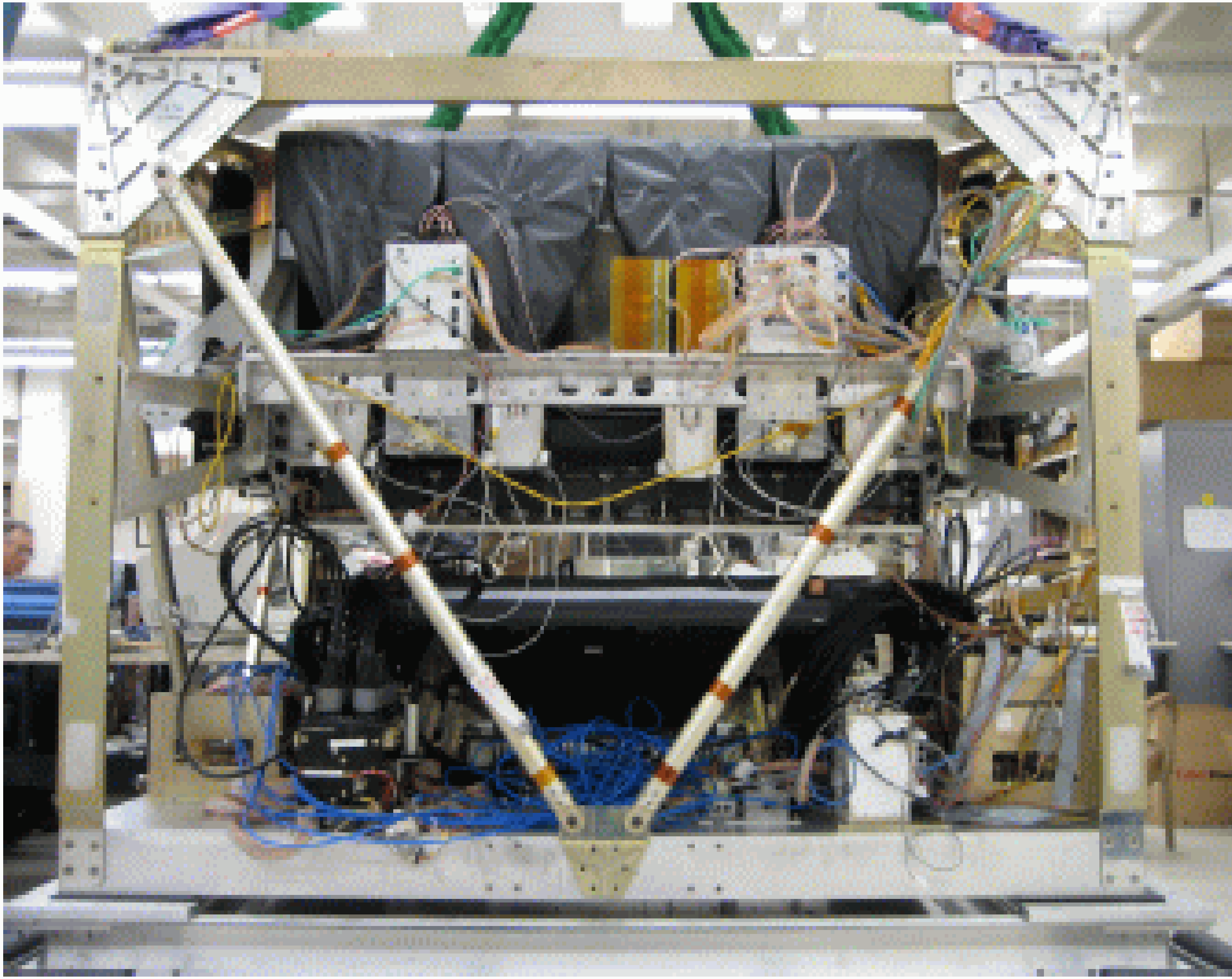

Two LDB flights to date: Average depth 3.9 gm/cm^2

CREAM I: 2004-05 42 days

CREAM II: 2005-06 28 days

Acceptance: 2.2 m^2 sr

Excellent charge resolution. Energy reach limited to below a PeV.
Multi-technique for energy measurement and intercalibration.

Direct calibration of energy measuring components and intercalibration in flight data from TRD and Calorimeter.

Charge Measurements: 2 layers of SCD

Park et al, Nucl. Instr. and Meth. A , 570, 286-291, 2007

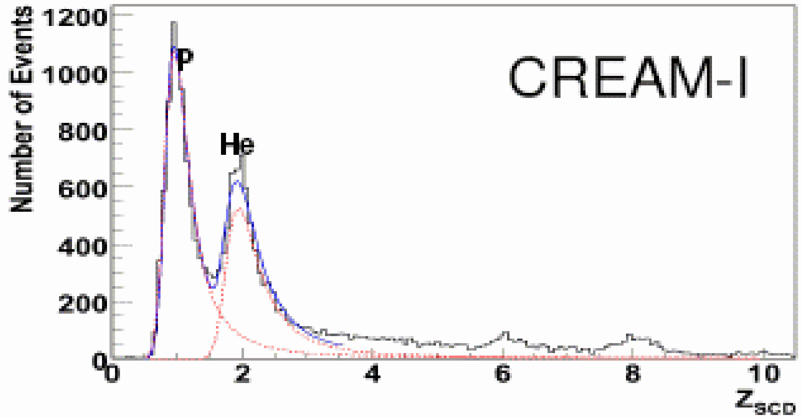

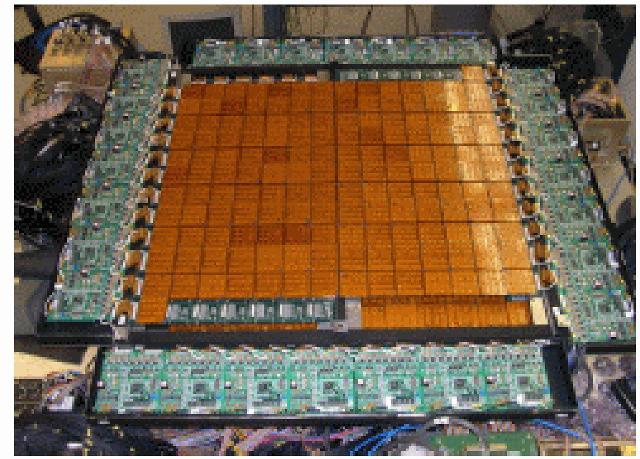

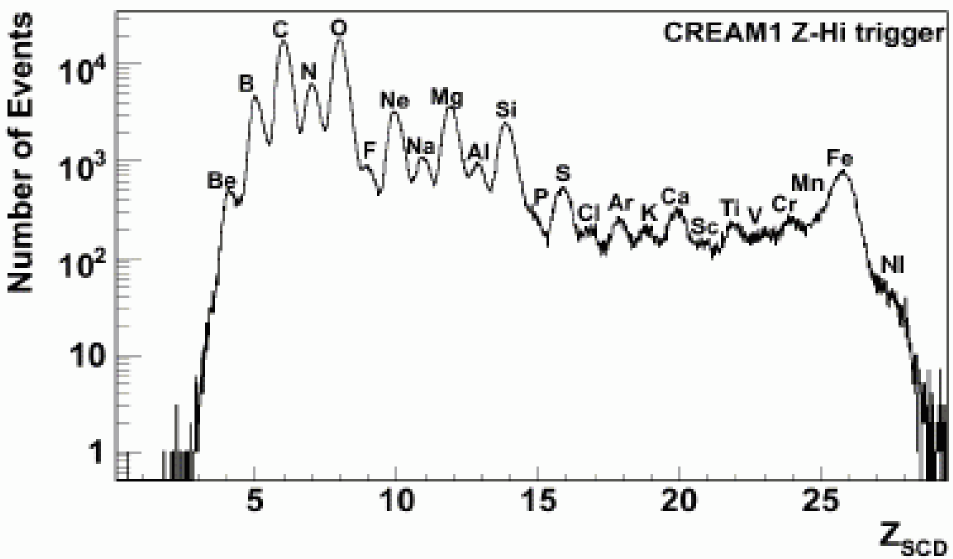

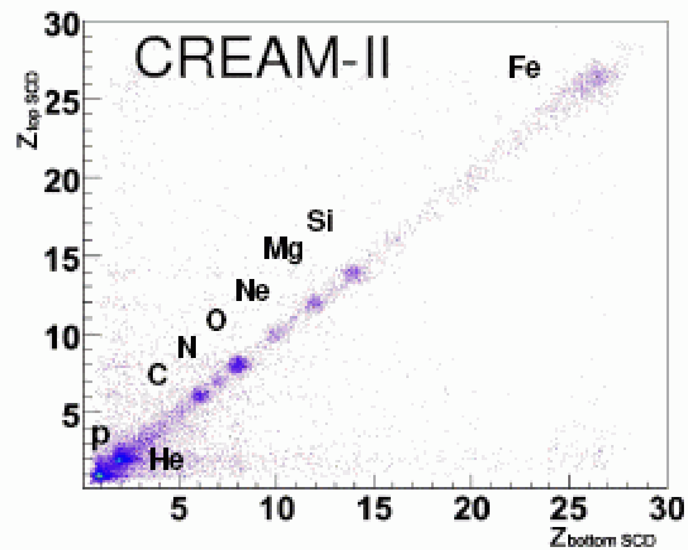

TCD charge measurement

Maestro, CREAM collaboration meeting Jan.11-12, 2007

Charge Resolution ~ 0.2 e for O and C

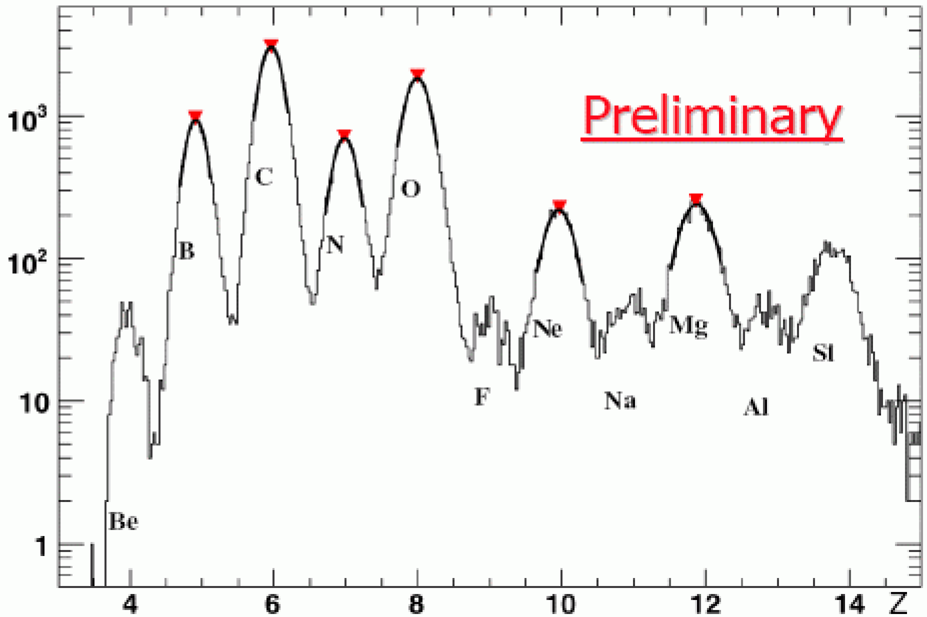

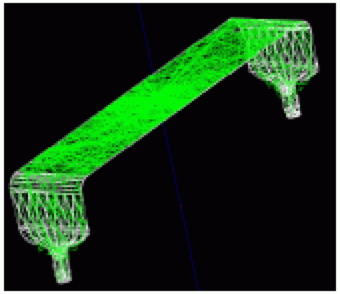

Spectrum of energy deposit (Prelim): Energy reach up to PeV

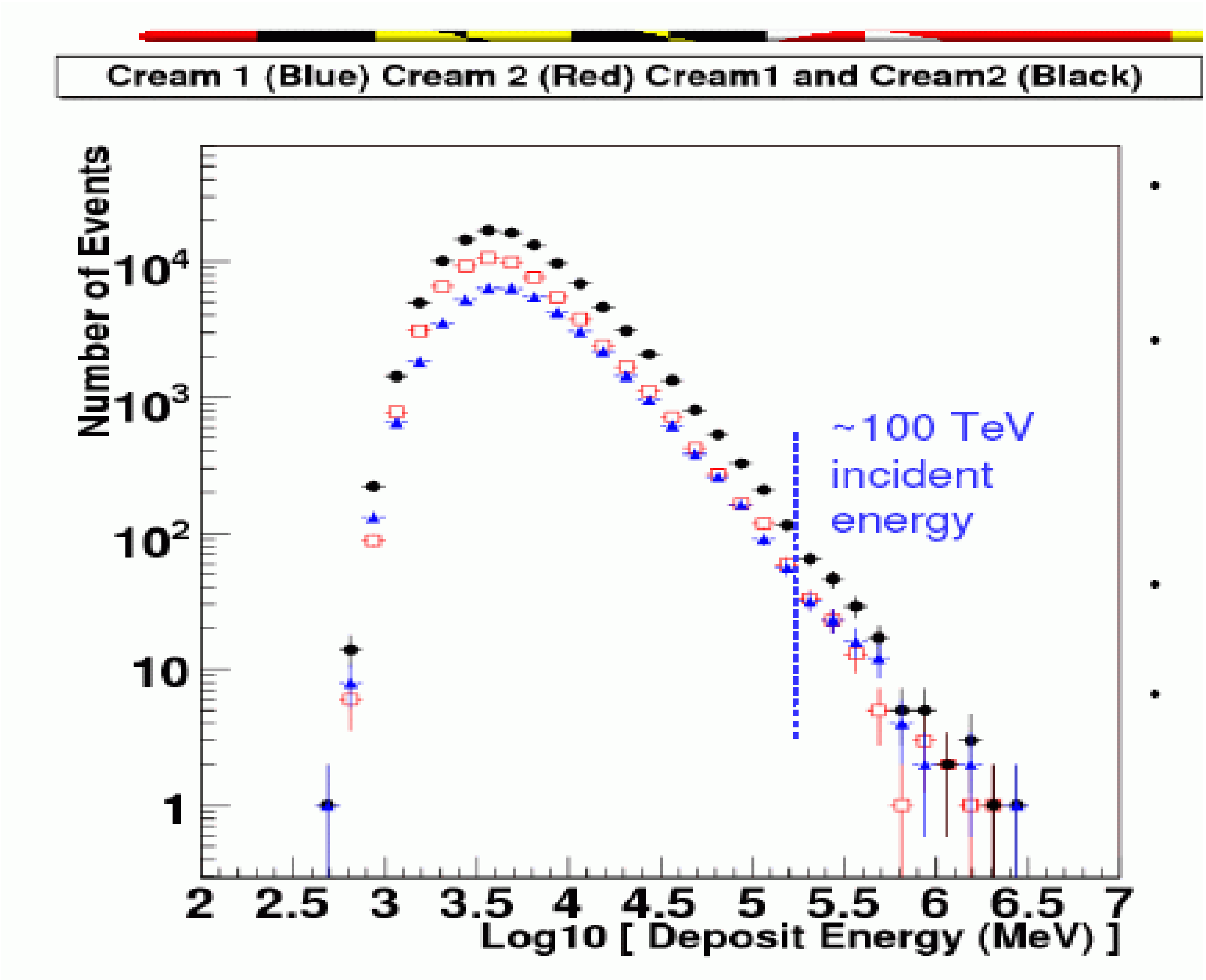

Energy Deposit for protons is steeper than for heavies

Seo et al. COSPAR, Beijing 2006

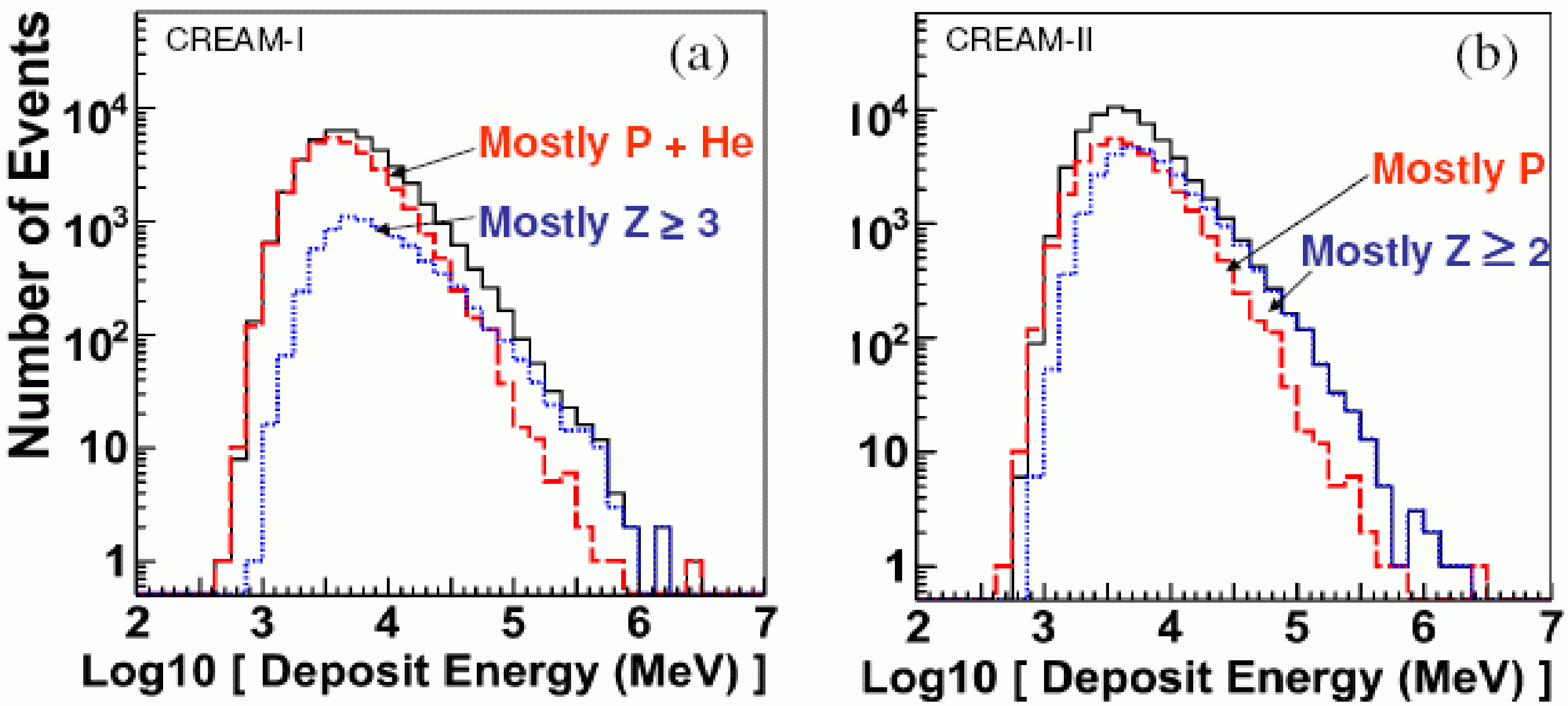

- Is this due to steeper proton source spectrum?
- Are the high energy protons lost preferentially due to the acceleration limit?
- Is this an artifact due to backscatter, leakage, or something else?

TRD results (preliminary) from CREAM and expected range

C & O spectra for 4 decades of energy

Wakely et al. COSPAR, Beijing, 2006

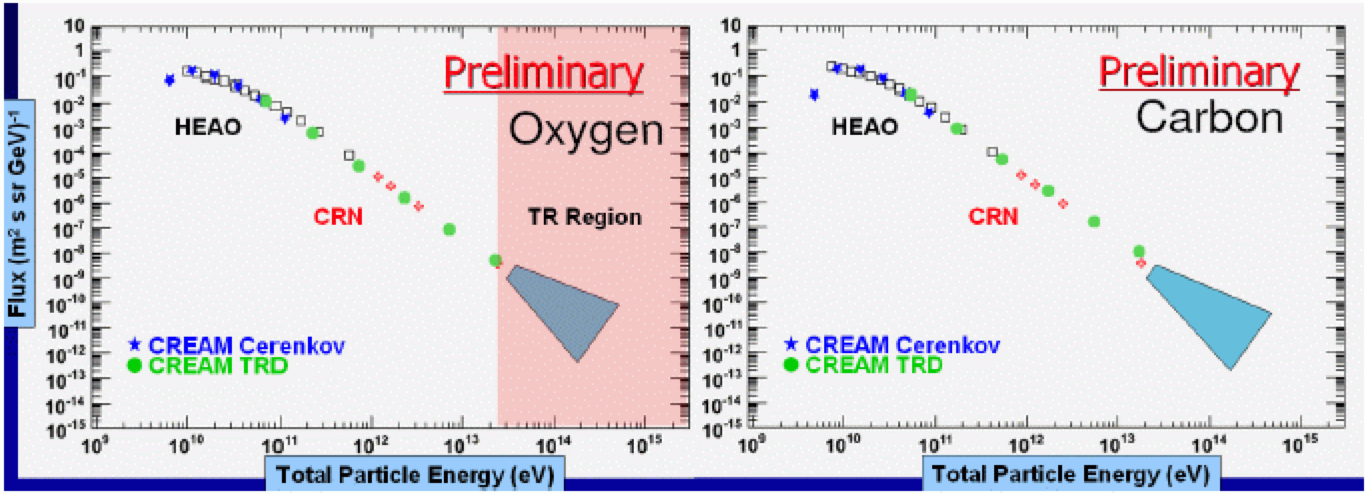

- Cuts: charge and velocity, pathlength, measurement stability etc.
- Spectral shapes agree with HEAO & CRN data at low energies and CREAM data extend to ~100 TeV
- No absolute flux: arbitrary normalization at the moment
- No atmospheric corrections yet

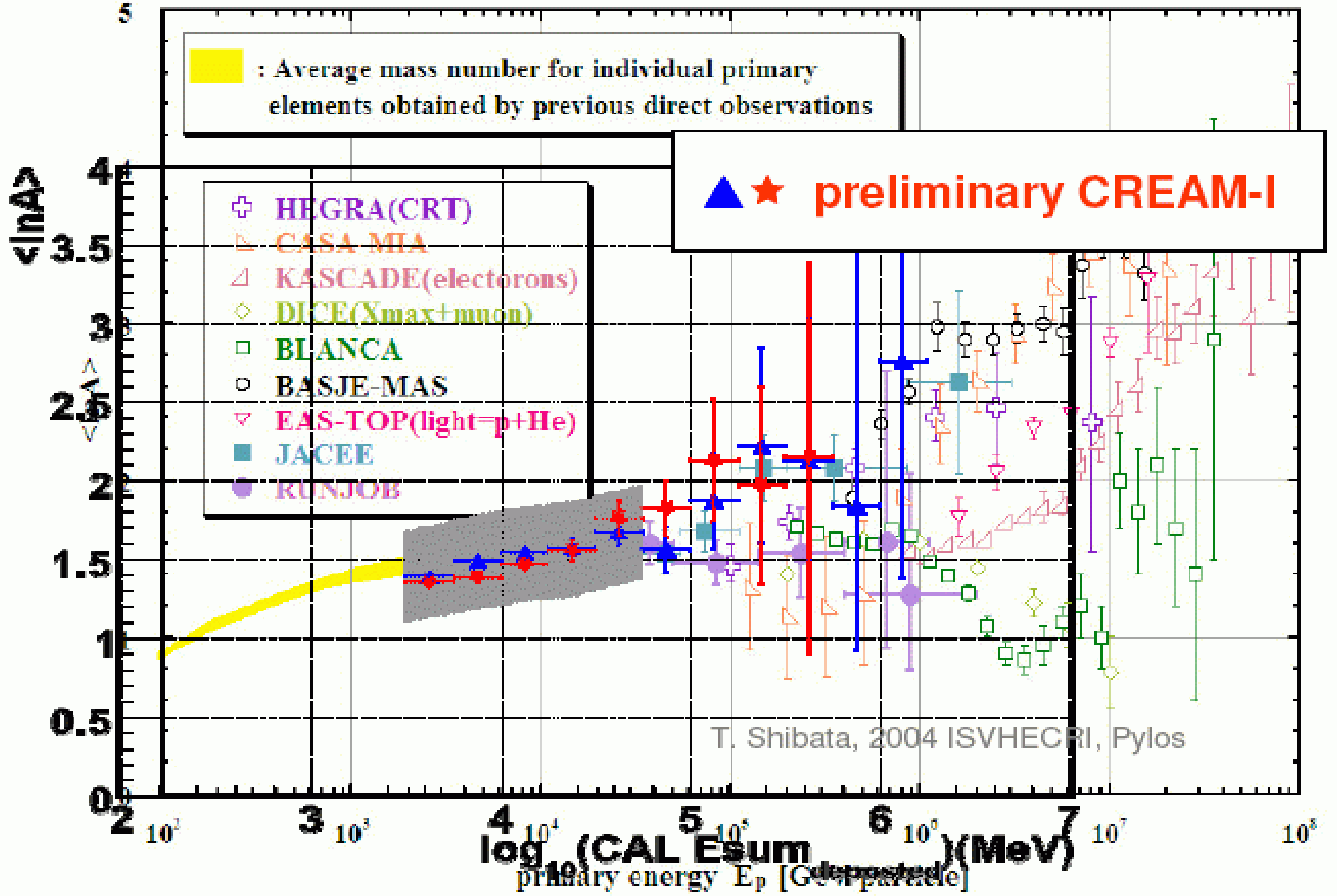
: Average mass number for individual primary elements obtained by previous direct observations
preliminary CREAM-I
HEGRA(CRT)
CASA-MIA
KASCADE(electorons)
DICE(Xmax+muon)
BLANCA
BASJE-MAS
EAS-TOP(light=p+He)
JACEE
RUNJOB
T. Shibata, 2004 ISVHECRI, Pylos
<lnA>
log10(CAL Esum deposited)(MeV)
primary energy Ep [GeV/particle]

Comments on the Composition figure:

1. From 5 TeV to 80 Tev reasonable agreement with previous measurements by JACEE and RUNJOB with <lnA> reaching 1.7 at 80 TeV

2. Above 80 Tev CREAM shows trend of JACEE, but cannot rule out RUNJOB.

3. Air Shower Nmu and Ne measurements from 100 TeV to 10 PeV(CASA-MIA, BASJE MUAS, and HEGRA CRT seem to continue trend of JACEE.

4. An increase of p and He favoured by EAS-TOP and KASKADE Ne

5. Difference in <lnA> of about 2 at 5 Pev between BLANCA and DICE and the results pointed out above in item 3.

My Conclusion:

Below 80 Tev Direct measurements are consistent

Above a PeV there is no agreement as to <lnA> amongst experiments using different techniques !!

Cosmic Ray Energetics And Mass (CREAM)

H.S. Ahn, O. Ganel, J. H. Han, K.C. Kim, M.H. Lee, L. Lutz, A. Malinin, E.S. Seo, R. Sina, P. Walpole, J. Wu, Y.S.Yoon, S.Y. Zinn
University of Maryland, USA
P. Boyle, S. Swordy, S. Wakely
University of Chicago, USA
N.B. Conklin, S. Coutu, S.I. Mognet
Penn State University, USA
P. Allison, J.J. Beatty, T. J. Brandt
Ohio State University, USA
J.T. Childers, M.A. Duvernois
University of Minnesota, USA
S. Nutter
Northern Kentucky University, USA
S. Minnick
Kent State University, USA
M.G. Bagliesi, G. Bigongiari, P. Maestro, P.S. Marrocchesi, R. Zei
University of Siena & INFN, Italy
J. A. Jeon, S. Nam, I.H. Park, N.H. Park, J. Yang
Ewha Womans University, S. Korea
M. Buénerd, A, Barrau, L. Derome, M. Mangin-Brinet,
Laboratorire de Physique Subatomique et de Cosmologie, Grenoble, France
R. Bazer-Bachi
Centre d'étude Spatiale des Rayonnements, Toulouse, France
A. Menchaca-Rocha
Instituto de Fisica, Universidad Nacional Autonoma de Mexico, Mexico
L. B. Barbier, J. Link, J. Mitchell
NASA Goddard Space Flight Center, USA

NEW

OBSERVATION OF DIRECT CHERENKOV LIGHT FROM PRIMARY IRON GROUP NUCLEI BY THE HESS EXPERIMENT IN 20 TO 200 TeV.

Method proposed by Kieda, Swordy and Wakely(2001)

Charge measured before nucleus breaks up
Energy measured after nucleus makes an air shower

My take on these results:

Iron Flux measured by H.E.S.S between 20 and 150 TeV agrees with that measured directly by JACEE and RUNJOB !

Hence the difference between different expeiments in this energy range for <lnA> must be due to disagreement about the spectra of light elements.

Principle of detection

Observation of Direct Cherenkov light from iron primaries by HESS. (Aharonian F. et al: Phys. Rev. D75, (2007), 042004)

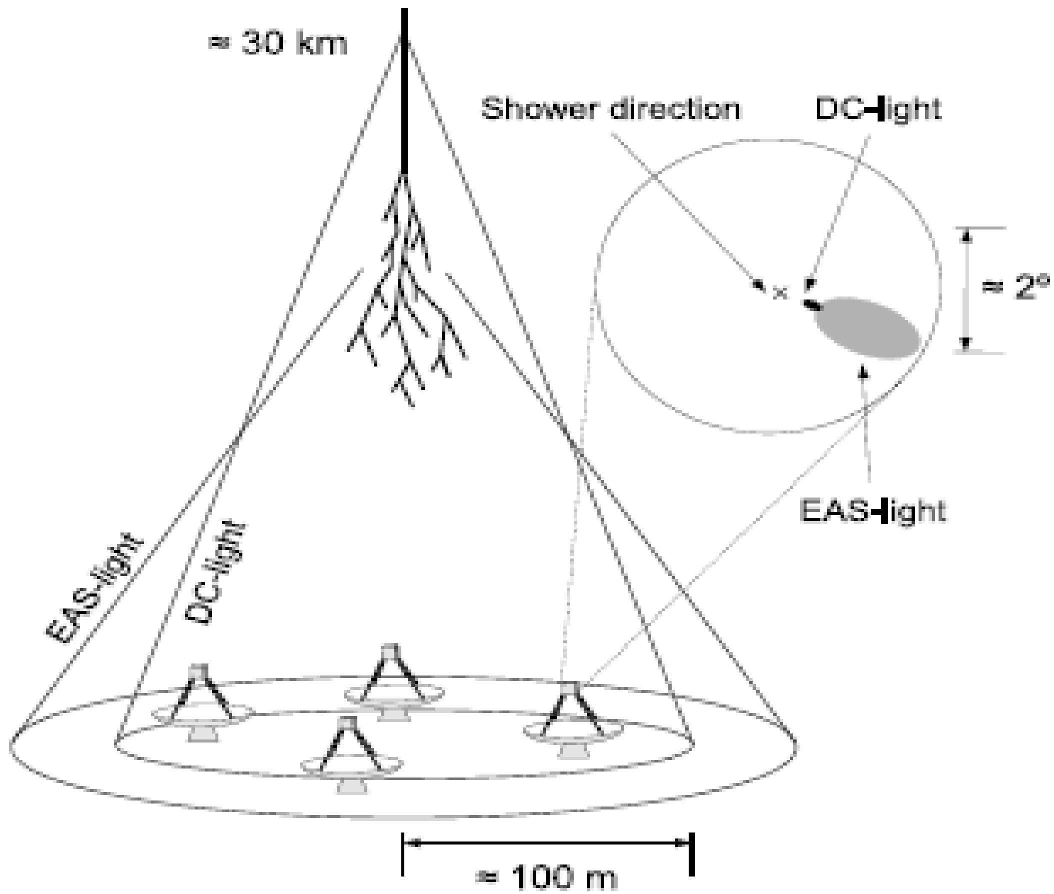

FIG. 1: Schematic representation of the Cherenkov emission from a cosmic-ray primary particle and the light distribution on the ground and in the camera plane of an IACT.

A Typical Event

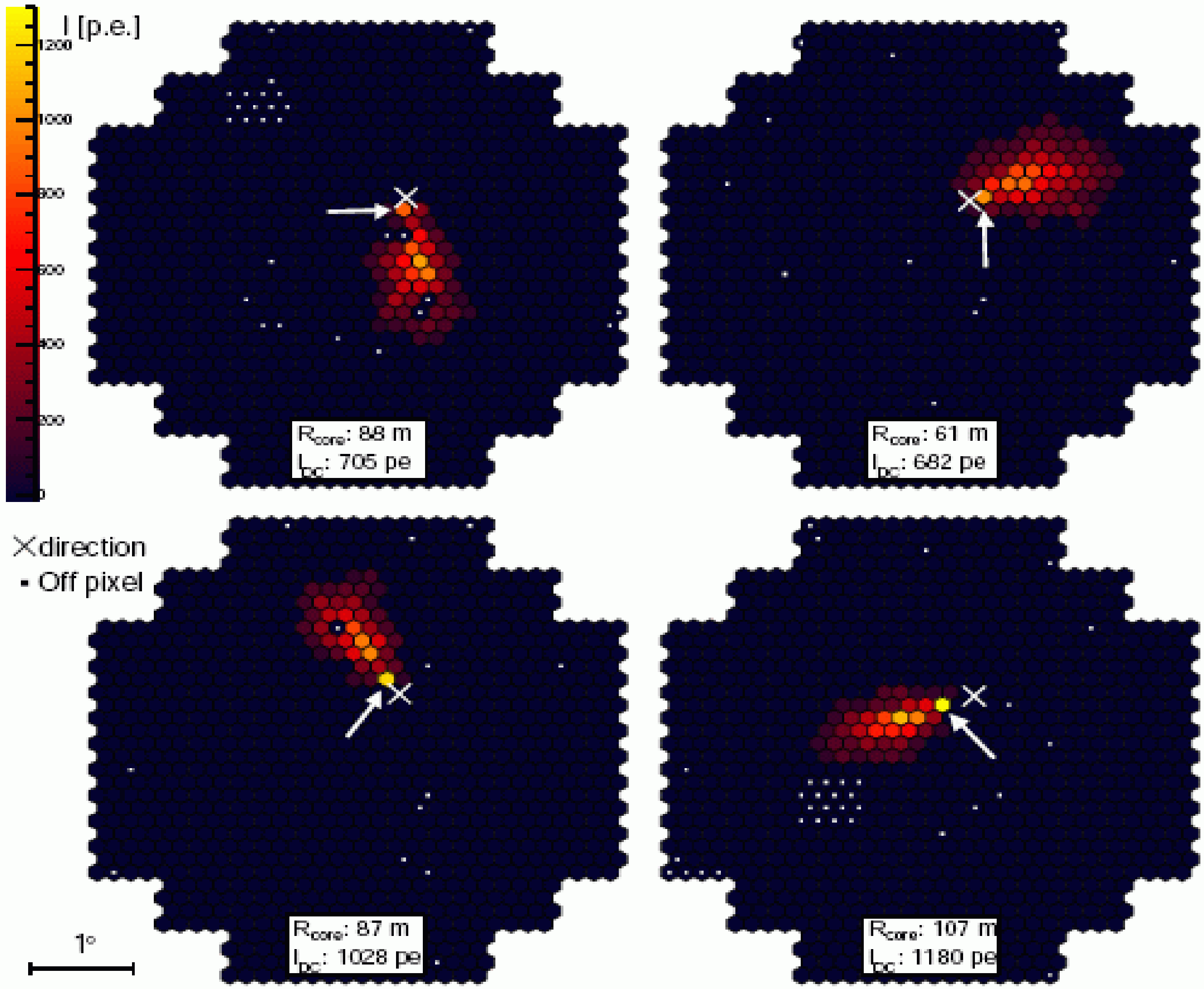

FIG. 5: A measured event with indications of DC-light in all four cameras images (indicated by arrows), after high threshold image cleaning. The reconstructed shower direction is shown by a cross (×) in each image. The reconstructed energy of this event is 50/48 TeV based on QGSJET/SIBYLL simulations. The reconstructed impact parameter and DC-light intensity for each telescope are shown in the lower panels in each image. The energy and impact parameter resolutions are ≈20% and ≈20 m, respectively. The white points mark disabled pixels.

Charge resolution for both hadronic models . Fluctuations in the first interaction depth limits the charge resolution at this time.

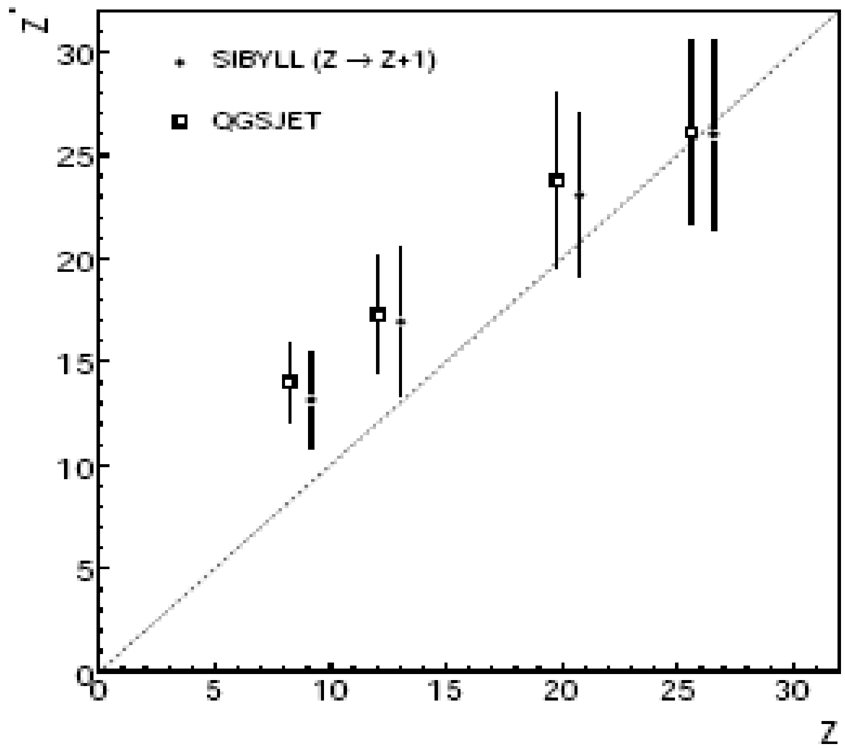

FIG. 7: Mean reconstructed charge Z^* as a function of the true charge Z for DC-events in an energy range of $1.5 < \log_{10}(E/\mathrm{TeV}) < 1.7$ for both hadronic models. For clarity the x-axis is shifted by +1 for SIBYLL. The error bars show the RMS of the distribution in each bin.

$$1.5 < \log_{10}(E/10\,TeV) < 1.7$$

Not sufficient for event by event charge assignment

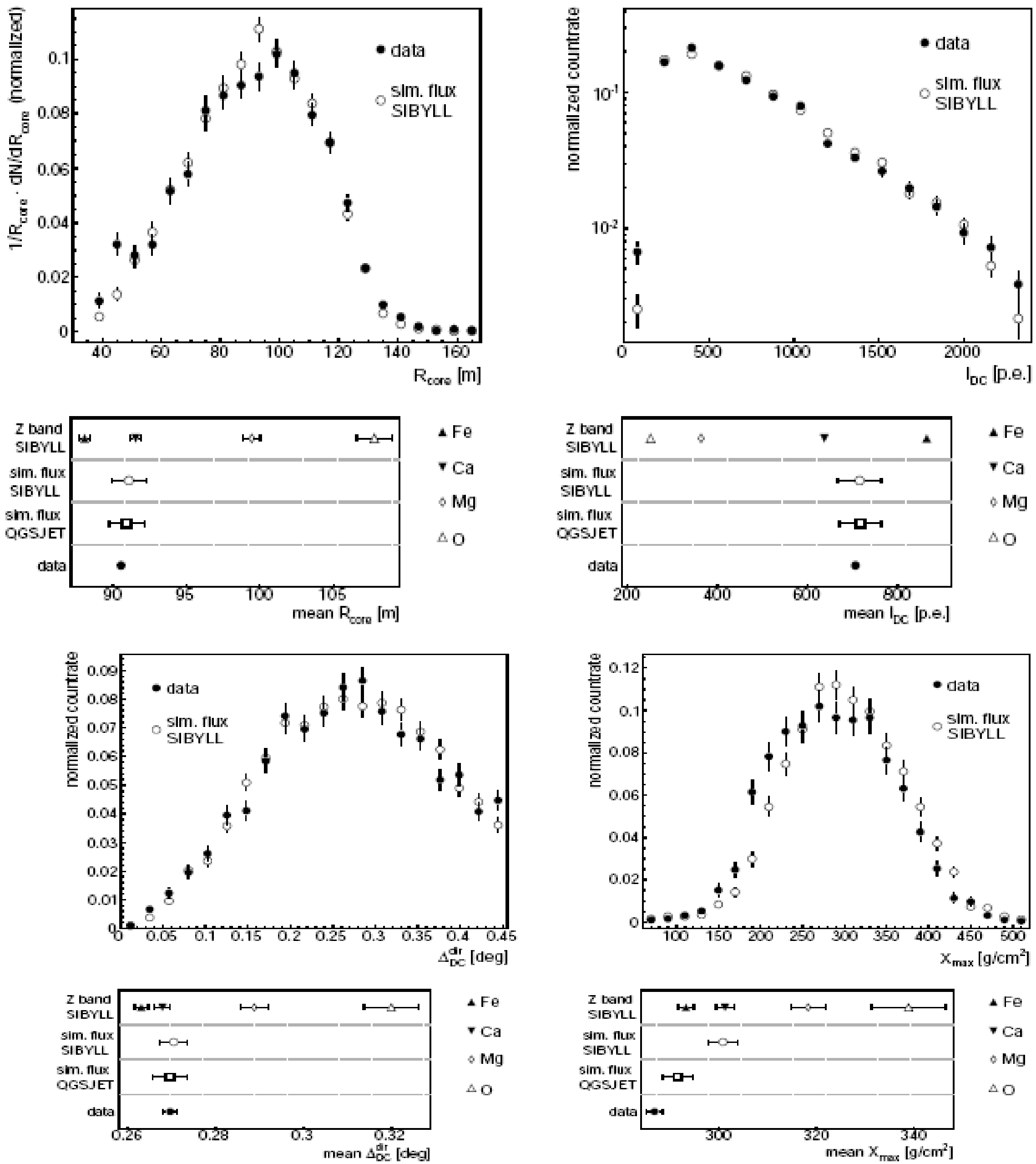

FIG. 8: Comparison of shower parameter distributions for data and simulations of the cosmic-ray flux. The bigger panels show normalized distributions of R_{core}, I_{DC}, Δ^{dir}_{DC} and X_{max} for SIBYLL simulations and data. The smaller panels underneath the distributions show their mean values and the mean value for the different charge bands of which the simulated flux is composed. Additionally, they show the mean value for the distributions for the QGSJET simulations. When comparing the mean values for the simulated fluxes one should bear in mind that roughly equal contributions to the error bars come from statistical errors and from uncertainties in the reference composition, which is the same for both models. The systematic difference between the mean values for the shower maximum X_{max} is not unexpected, since this quantity is difficult to treat in the simulations (see text).

Find the fraction of Fe events by fitting observed distributions to simulations. A two component model used : Fe + remaining nuclei. Relative fractions of remaining nuclei kept fixed iron fraction only variable.

Fe fraction increases with energy for both Sybll and QGSJET models. From about 0.5 to about 0.8 for log_10(E/TeV) from 1.1 to 2.3.

Measurement of the Fe spectrum between 15-200 TeV

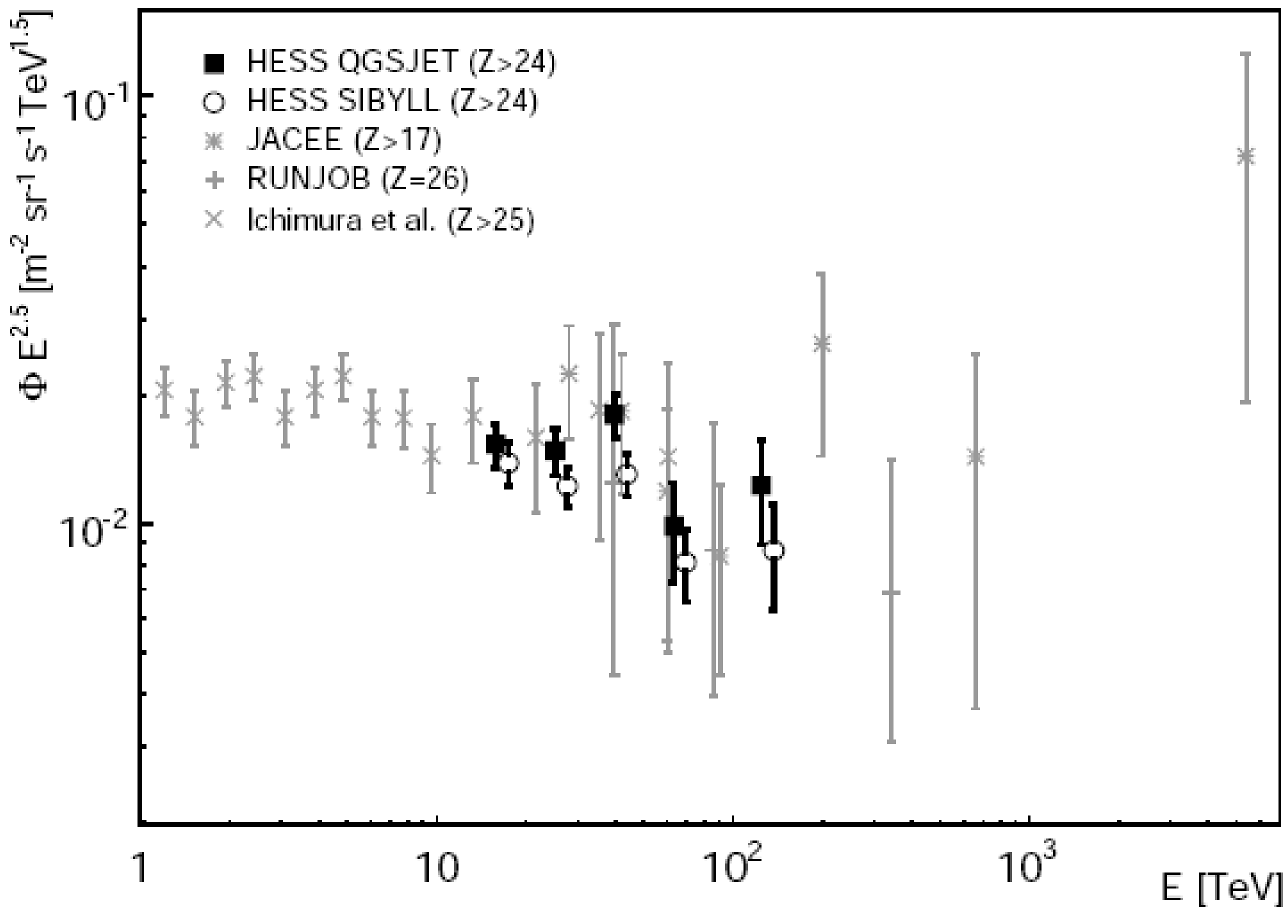

FIG. 10: Differential iron energy spectrum measured with H.E.S.S. for the hadronic models QGSJET and SIBYLL multiplied by $E^{2.5}$ for better visibility of structures. The spectral points for both models are measured for the same energies. For better visibility the SIBYLL points were shifted 10% upwards in energy. The error bars show the statistical errors. The systematic flux error in each bin is 20%. The measurements from balloon experiments with data points at the highest energies are shown for comparison [8, 25, 26] (a compilation with more measurements from balloon experiments and space born measurements can be found in [1]). For a better visibility no horizontal bars marking the bin ranges are shown, they can be found in the respective papers. When comparing the measurements one should bear in mind that the experiments have different charge thresholds for their definition of the iron band (see legend).

Cannot as yet distinguish between JACEE and RUNJOB

Many TeV “ gamma ray “ sources in the galactic plane discovered by HESS and MILAGRO since Aspen 05

A brief partial summary

Many galactic sources generating TeV gamma rays – associated with PWN, SNR and UID EGRET sources. Certainly some are sources of nuclear cosmic rays. Gamma ray yield for diffuse emission within a factor of few of GALPROP calclations.

No unique identification of acceleration of nuclei in these sources.

Results from ground based telescopes for TeV gamma-ray observations:

HESS results on Galactic Center Ridge: Nature:(2006),**439**,695

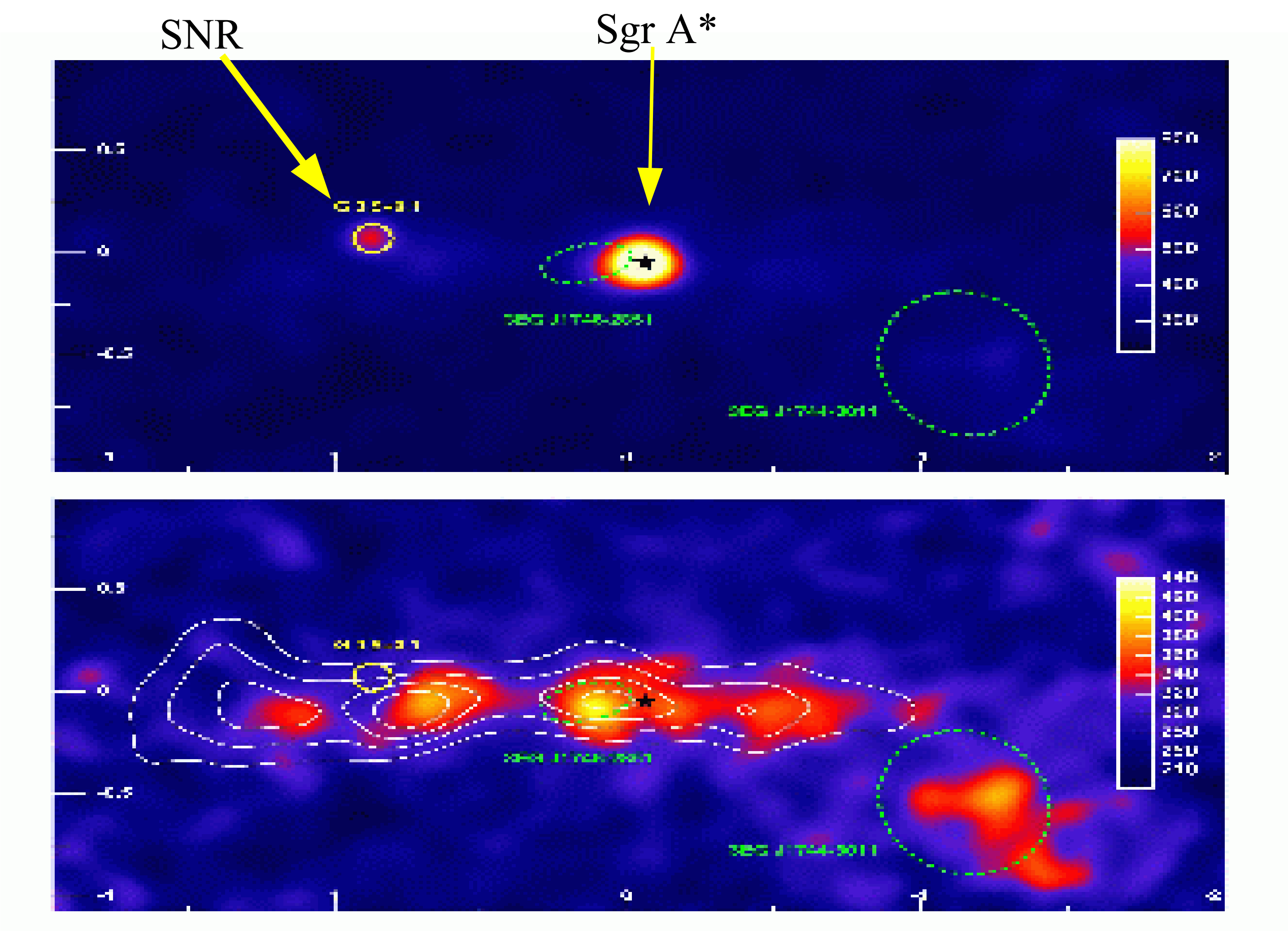

1 0 -1 galactic longitude

Bright suources subtracted.

White contours molecular gas (CS emission)

Gamma ray emission – histogram ; red curve: molecular gas

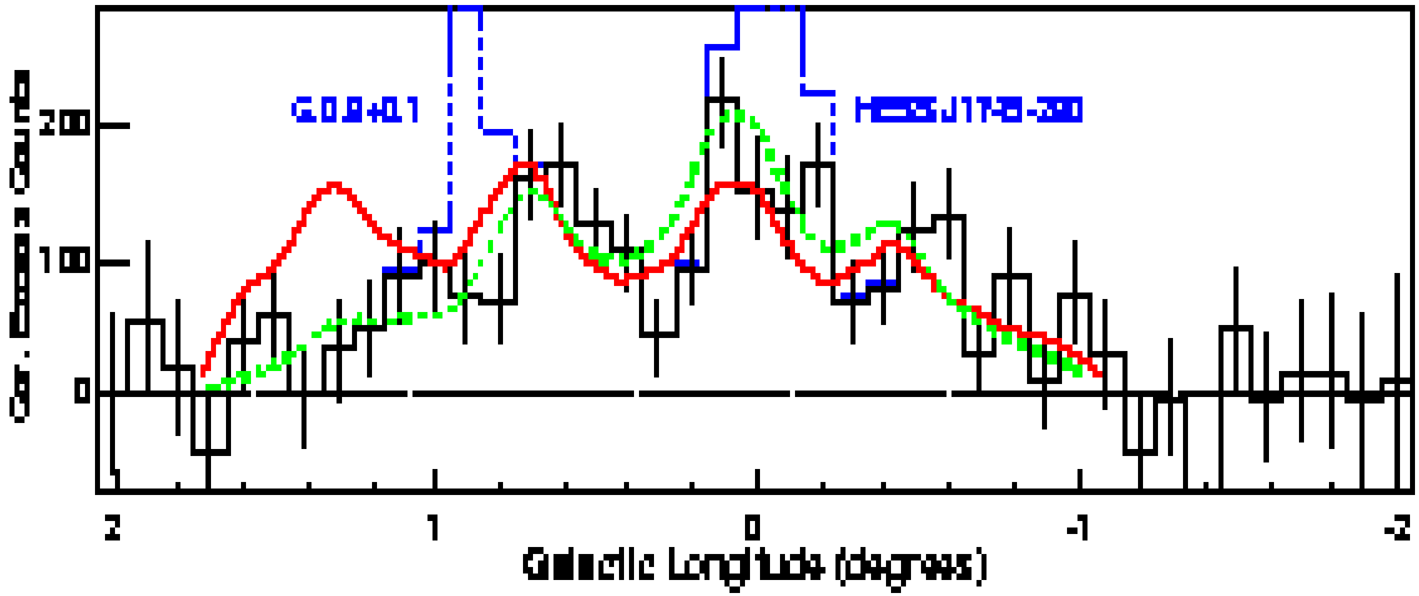

Green dashed line: calculated gammas from CRs diffusing away from a central source of age 10^4 yrs

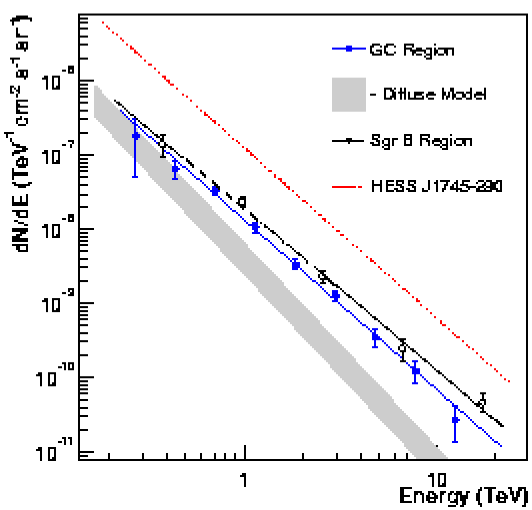

Shaded band: diffuse emission expected for CR flux with density and spectrum same as near earth spectrum. Indicative of contribution due to local sources.

HESS galactic plane survey -30< l < 30 and -3<b<3

Aharonian F, et al; Ap.J.(2006),**636**,777

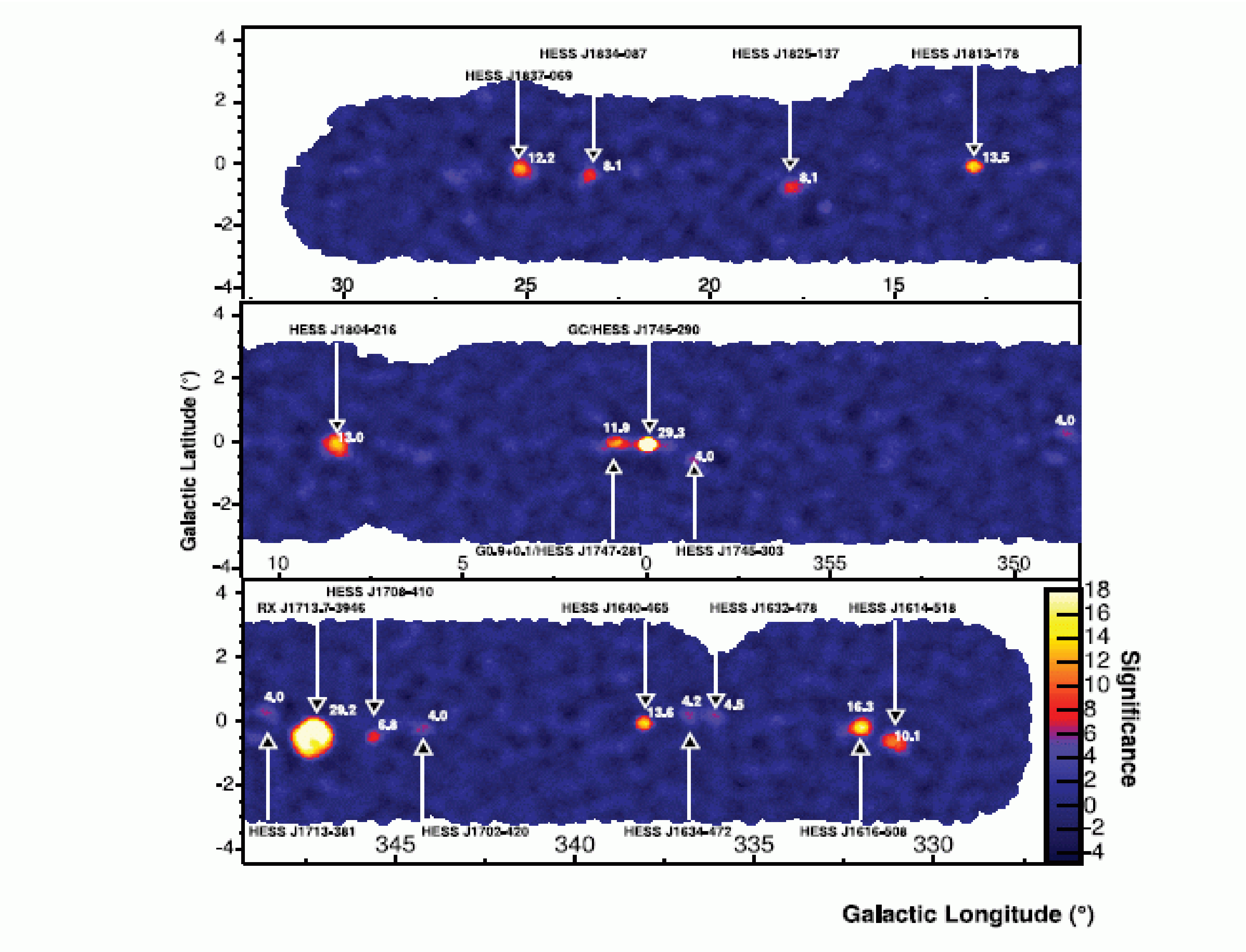

15 TeV sources – correlated with energetic objects – seen in other bands

Some Milagro results of galactic plane

Shown at Median energy 12 TeV

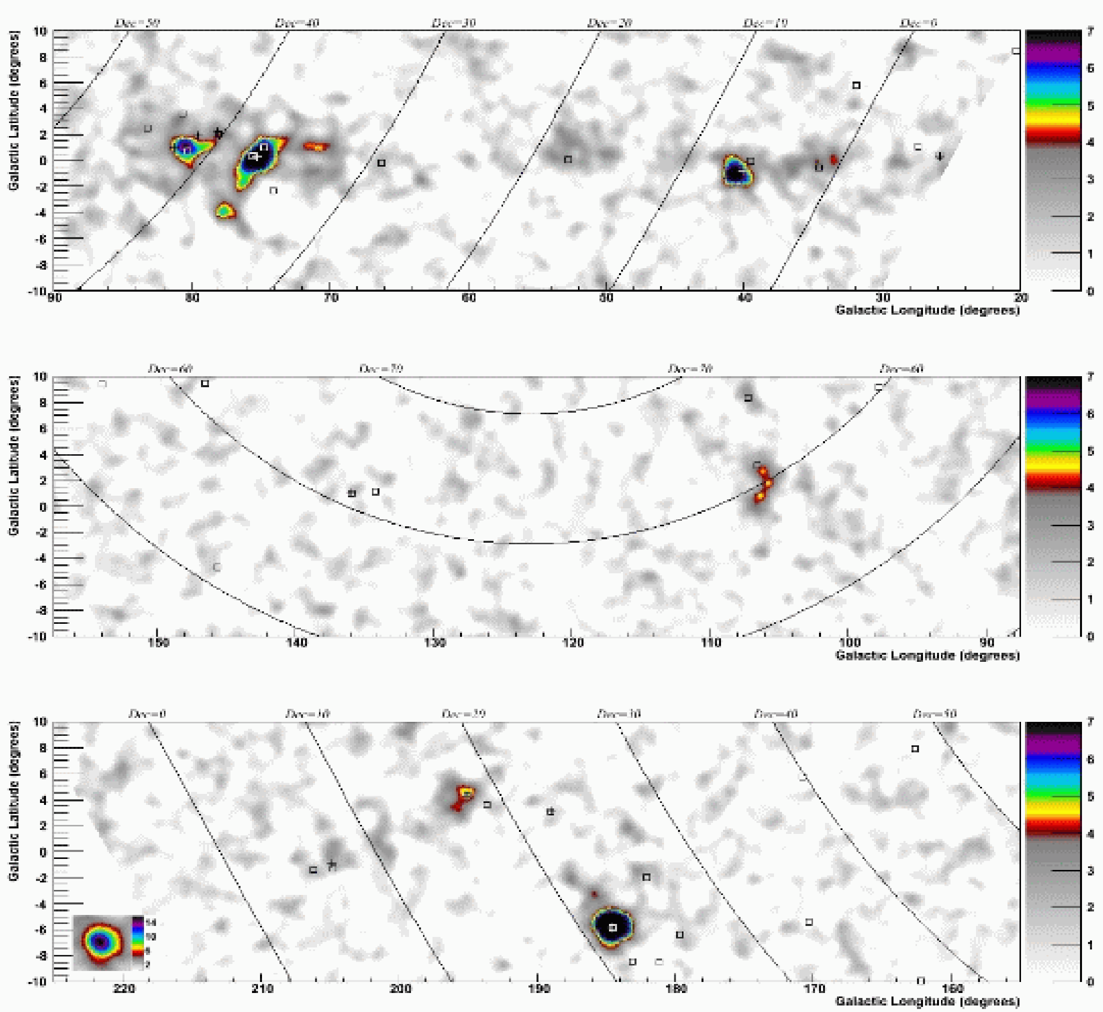

Milagro's view of sources in the Galactic plane with a median energy of 12 TeV. Colors are significance (above 4.5 σ pretrials). Squares are from the 3rd EGRET catalog while the crosses are from the EGRET GEV catalog. Our point spread function (from Crab data) is shown in the lower left corner

$-30 < l < 220$
(different from HESS)
$-10 < b < 10$

“> 5 “ new TeV sources + diffuse emission and extended sources

Aous Abdo,et al: Ap.J. Being submitted(2007)

Diffuse gamma-rays imply CR intensity which is not the same over the whole galaxy at multi-TeV nergies.

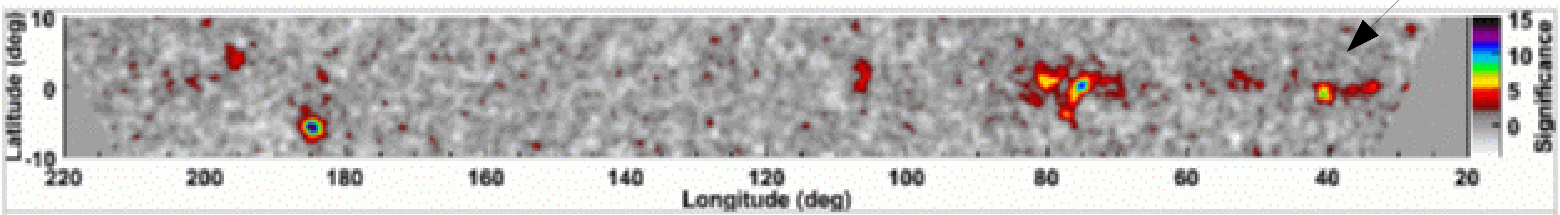

Figure 2. Significance map of the Galactic plane visible to Milagro. There are 7 interesting spots of TeV gamma-ray emission with > 4.5 standard deviations within |*b*| <

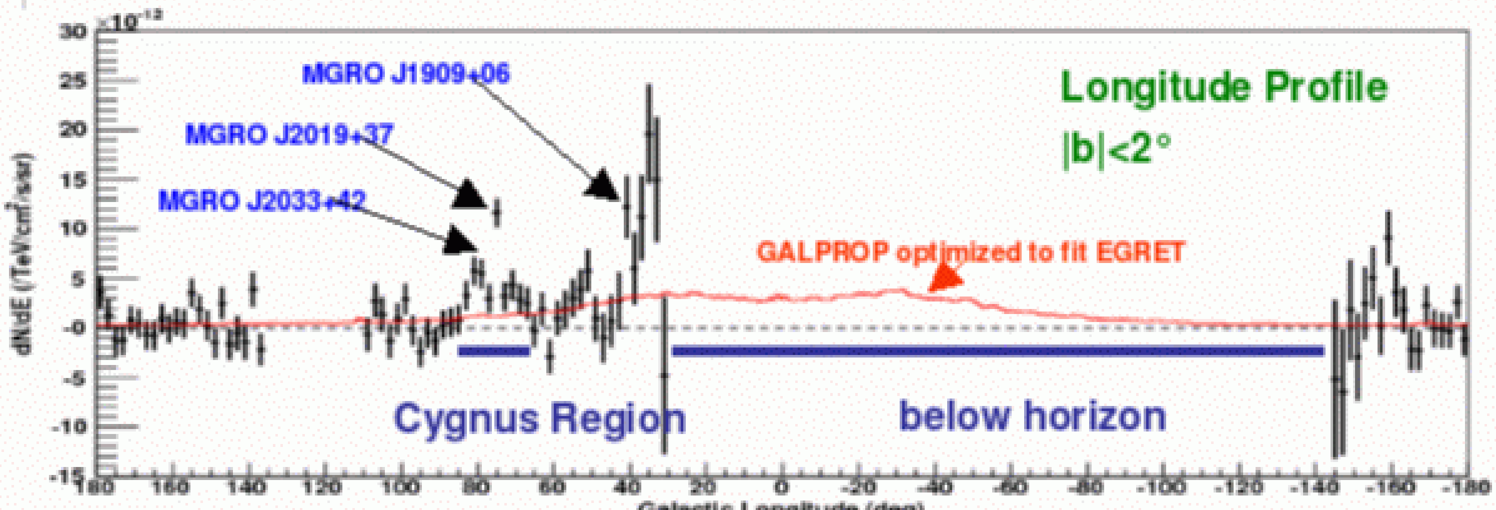

Figure 3. Milagro's measurement of the longitudinal profile of the galaxy with |b| <2°. The overall excess in the Cygnus region can be seen as well as the three new sources discovered by Milagro. The red line is the GALPROP fit to EGRET data. This is the first measurement of this type above 1 GeV.

R. Atkins, et al: Phys. Rev. Letters; 95(2005)251103

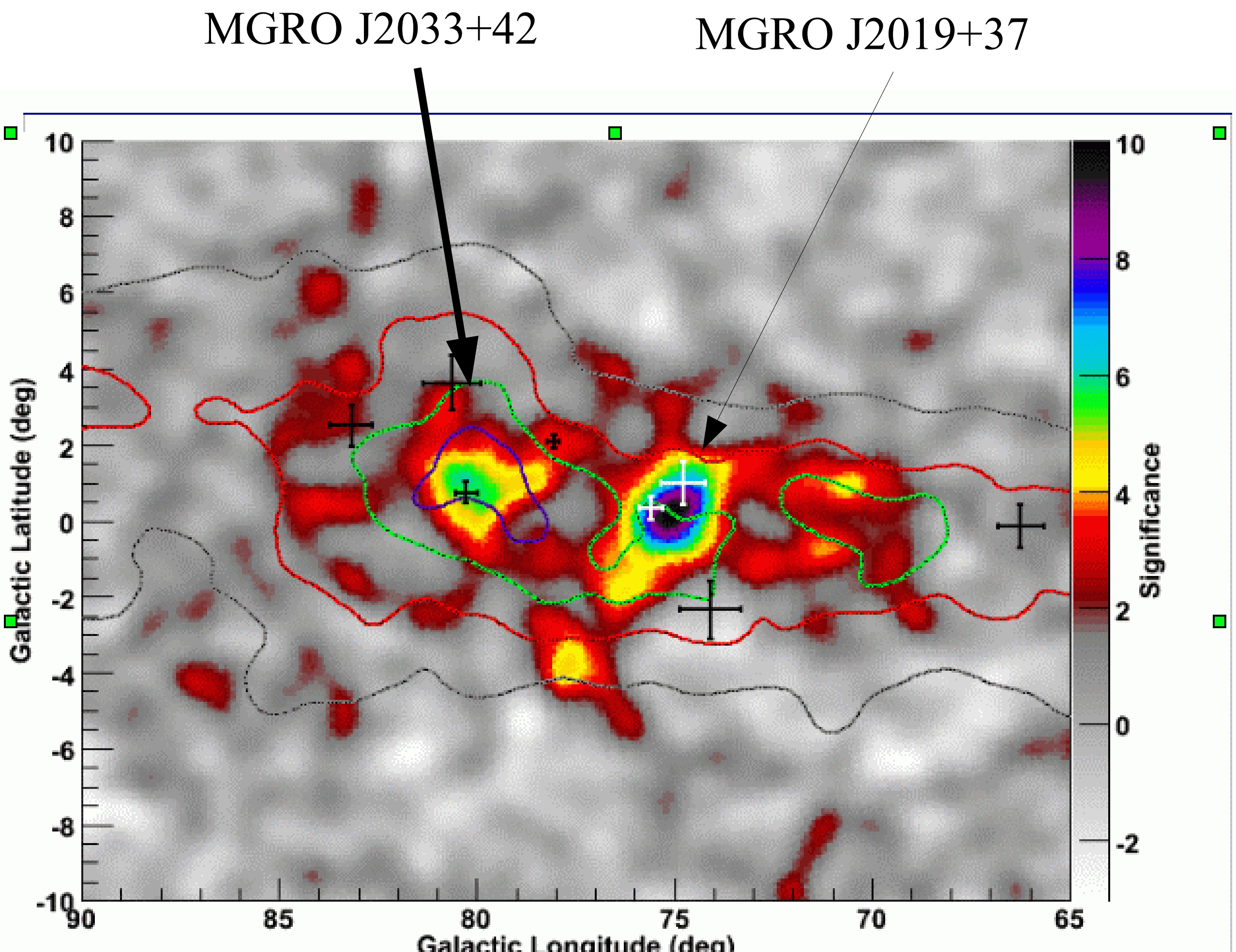

Figure 4 – The Cygnus region as seen by Milagro shown with contours of expected π^0 produced gamma-rays s predicted from the GALPROP model with no sources. The crosses are unidentified EGRET sources. Figure from [2]

A. Abdo, et al: Ap.J. Letters, 658(2007)L33-L36

TeV: A New Window on the Sky

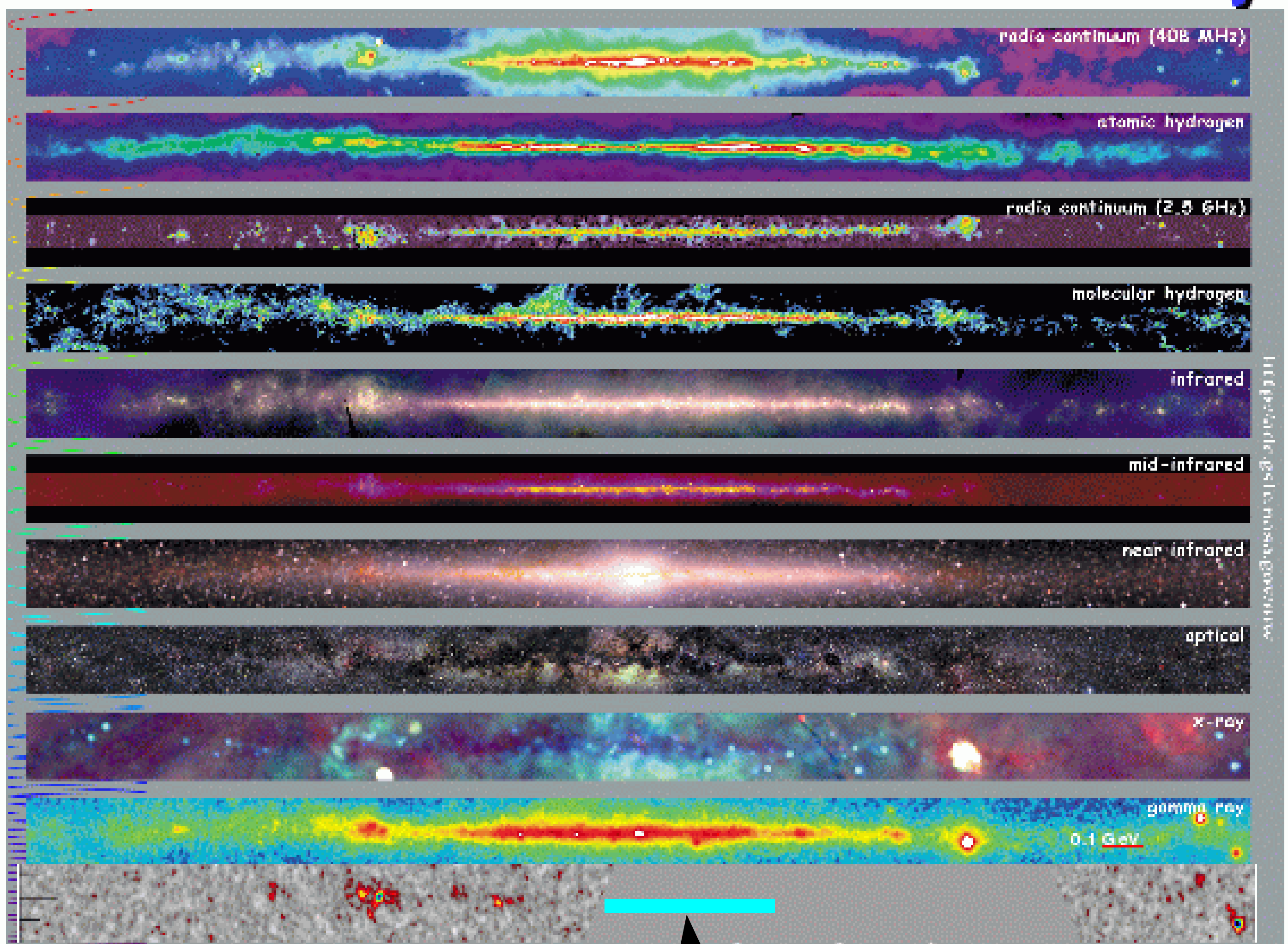

Milagro

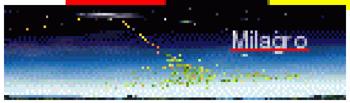

HESS

Hess covers the center of the galaxy region

NEW

Measurement of coherent radio emission from air showers: LOPES + KASKADE

Coherent geosynchrotron radiation.

1. Signals scale approximately linearly with energy
2. Low frequency radio emission favorable
3. Electric field strength decreases exponentially with distance from the core.
4. Can operate for all 24 hours
5. Inclined showers favorable.

Radio Emission: Lopes and KASKADE

Horneffer et. al.;Int. Journal of Modern Physics A, vol 21, supplement 1(2006) 168-181;
Falcke H, et.al.; Nature(2005),**435**,313.

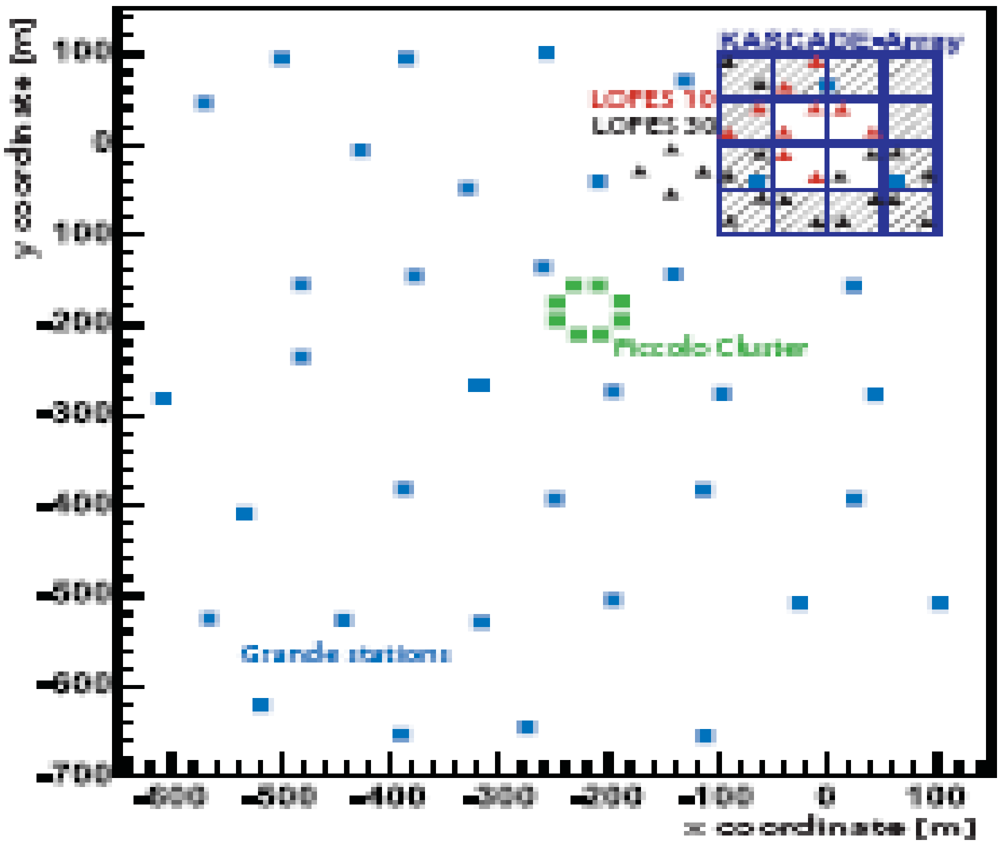

Figure 4. Layout of the LOPES10 and LOPES30 array configurations relative to the KASCADE-Grande surface detector components.

Antenna

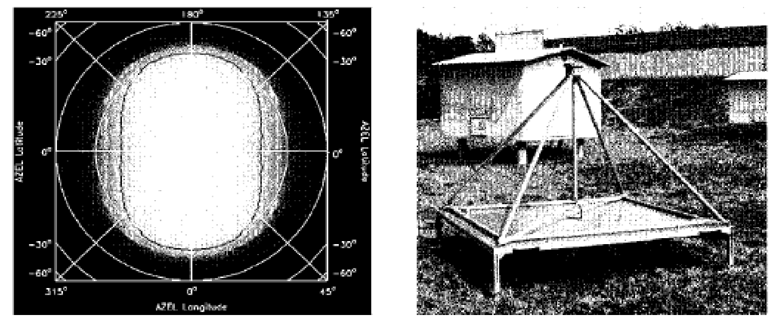

Figure 6. Left: Gain pattern of a single LOPES antenna. The vertical direction (azimuth = 0° or = 180°) is the direction perpendicular to the dipole, the horizontal direction is the one parallel to the dipole. The contours are at the 50% and 10% levels. Right: One of the LOPES antennas at the KASCADE-Grande site.

30-240 MHz

LOPES 30

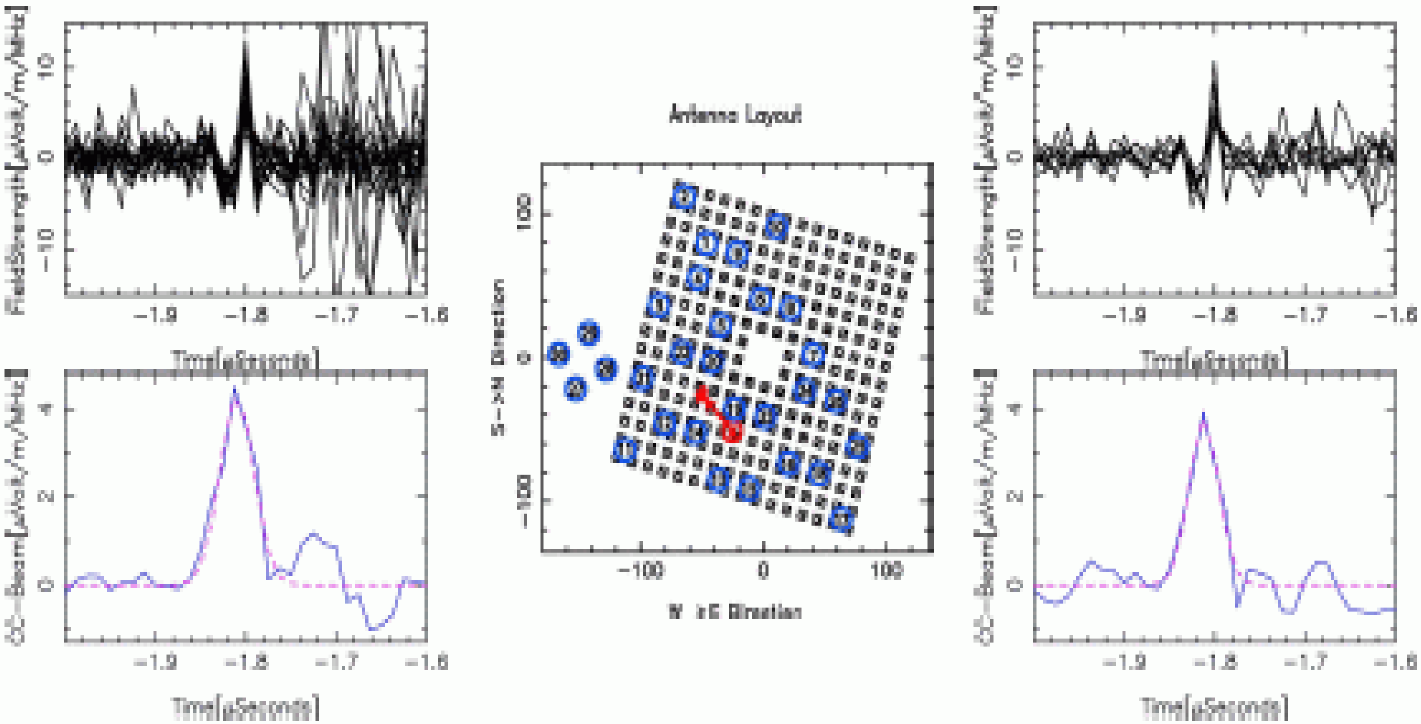

Figure 2. Example of an event registered by LOPES-30. Left: Field Strength of all individual 30 antennas and the result of the Cross Correlation(CC)-beam forming (Full line: CC-beam. Dotted line: Gaussian fit). One can clearly distinguish between the coherent radio pulse at -1.8 μs and the detection of incoherent RFI from KASCADE at -1.7 μs. Middle: Antenna layout at the KASCADE array. The arrow indicates the direction of the incoming cosmic ray shower of this event. Right: The same event reconstructed by using only a selection of antennas (antenna numbers from 1 to 10, see layout) and the resulting signal. For antennas positioned further from the shower core there is a less noise coming from KASCADE (detector stations), and also the resulting CC-beam value is 12.5 % weaker than the value obtained by all antennas.

Shower direction to better than 0.1 deg with core location from EAS.

LOPES/KASKADE correlation:

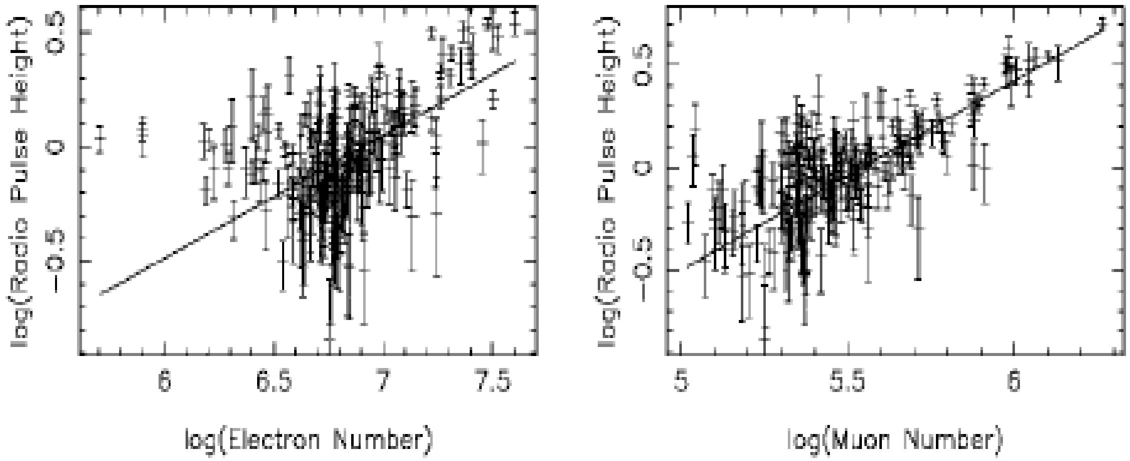

Figure 3. Normalised radio pulse height after scaling by the fit to the geomagnetic angle and distance to the shower axis. Plotted against the electron number (left) and muon number (right).

Small zenith angle   Inclined showers

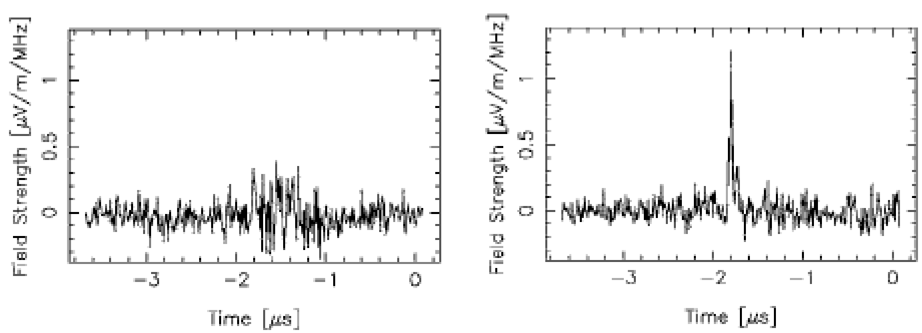

Figure 4. Left: Sum over the formed beams of the eight least inclined air showers in the selection. Right: Same sum but over the eight most inclined air showers. The average muon number in both groups is ca. 3×10^5.

LOFAR array under construction – detecting and measuring cosmic ray showers above the knee without the aid of an EAS array ? How wide an energy range can be measured in a single experimental arrangement ?

Some Comments about Cherenkov experiments

A list of experiments

- HEGRA CRT
- DICE
- BLANCA
- CACTI
- TUNKA

Energy measured through Cherenkov yield at large distance from core of shower + simulations

Xmax estimated thru measurement of Cherenkov LDF hardness: C(r1)/C(r2)

Cherenkov array : TUNKA and recent developments.

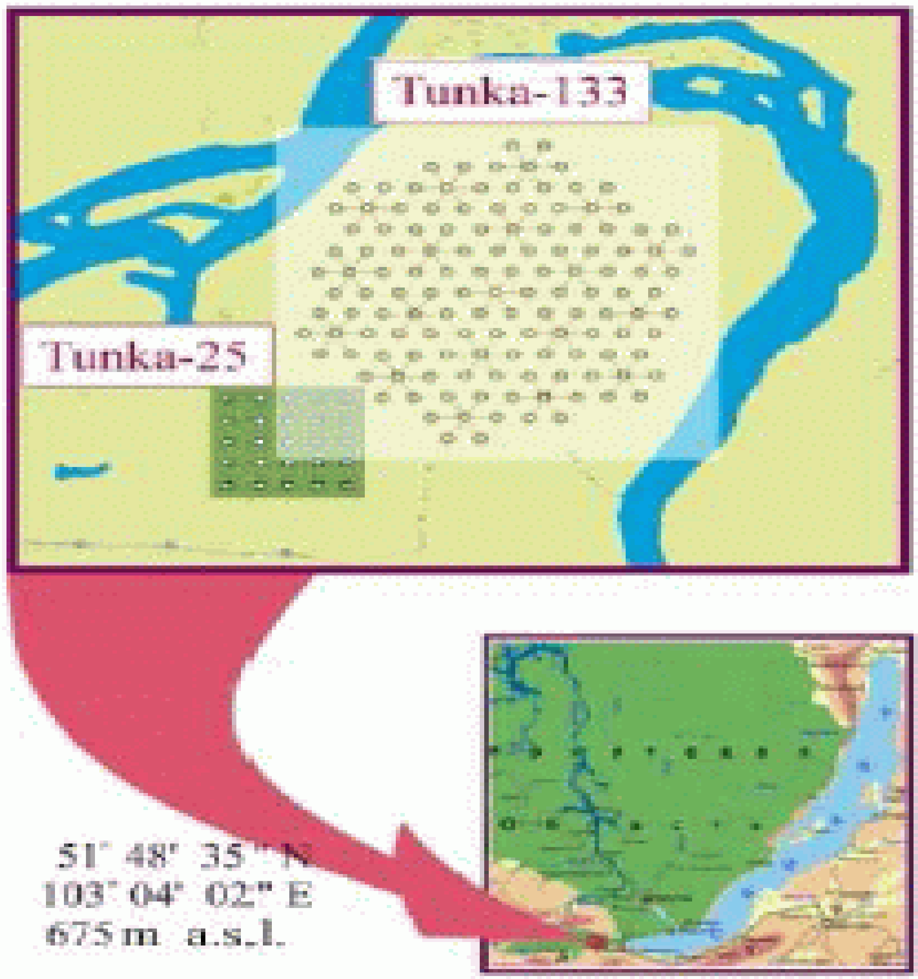

Figure 1. Location of Tunka-25 an the proposed Tunka-133 array.

Papers at ICRC Pune(2005) and Int. Journal of Modern Physics A(2007)

TUNKA Energy spectrum and Xmax

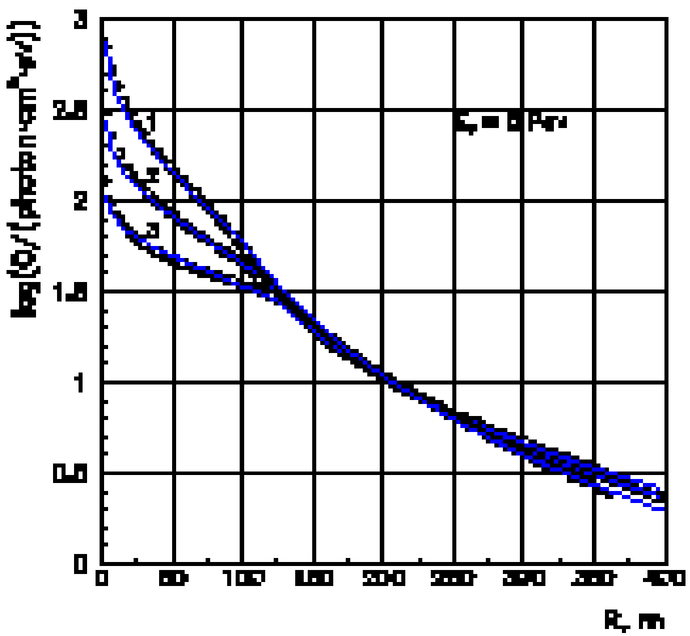

Figure 1. CORSIKA EAS Cherenkov light LDFs and fitting functions. 1 - P = 5, 2 - P = 4, 3 - P = 3

Measure Cherenkov LDF.

Energy from absolute intensity of Cherenkov light at 175 m from core and simulations

$$E_0(TeV) = 400\, Q_{175}^{0.95}$$

Xmax from steepness P and simulations.

$$P = \frac{Q(100)}{Q(200)} \text{ and}$$

$$H_{max}(km) = 17.63 - 0.0786 \times (P + 8.917)^2$$

TUNKA 25 spectrum

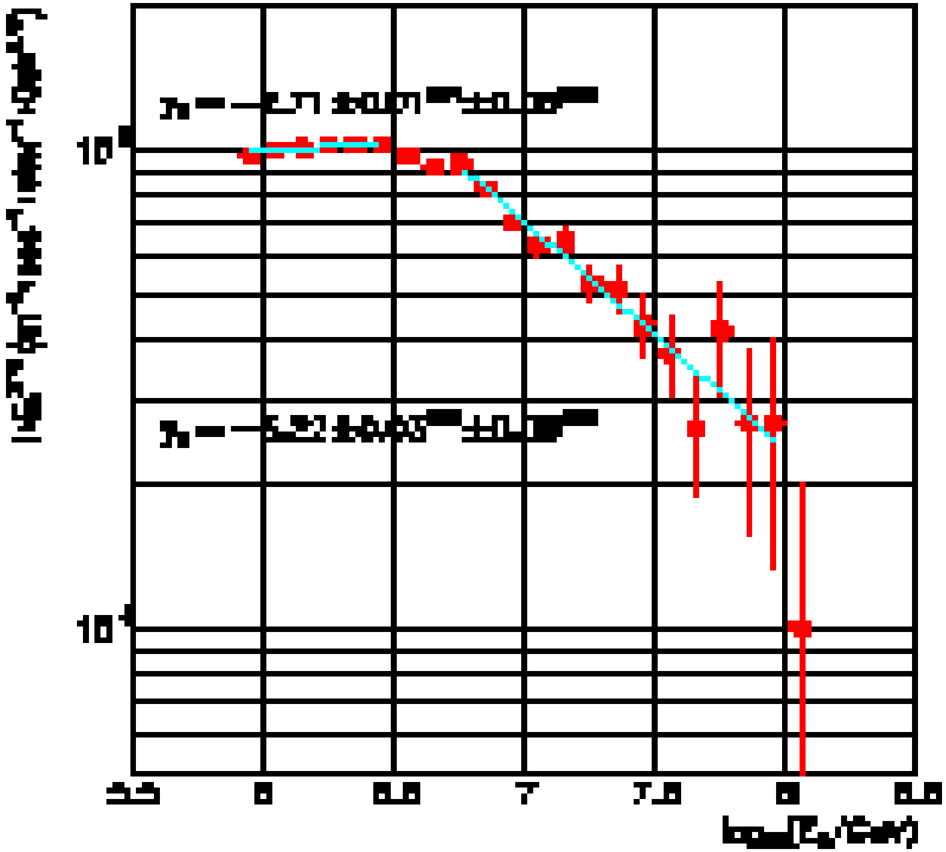

Figure 2 EXPERIMENT: Differential energy spectrum.

Xmax and composition analysis

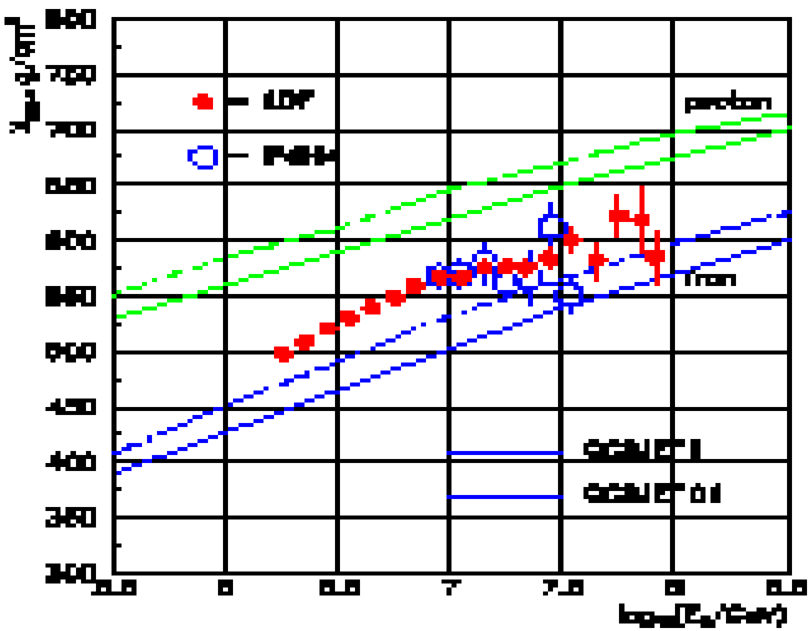

Figure 3. Mean depth of EAS maximum vs energy.

Elongation rate and actual value compared with simulations.

Fluctuations compared with simulations of diff. species

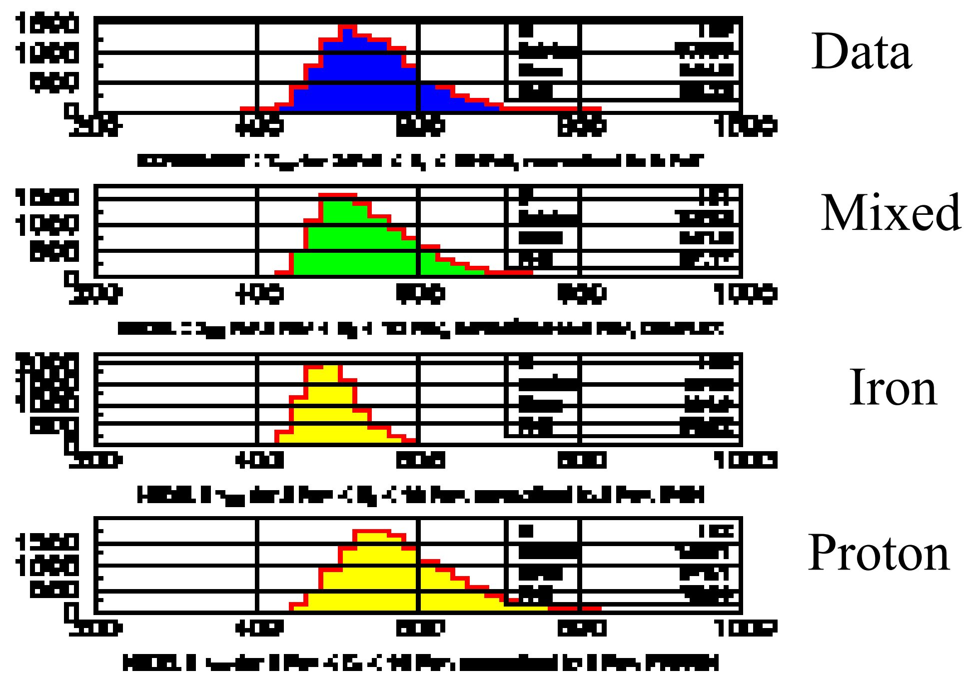

Figure 4. X_{max} distribution.

Other Techinques for energy and composition extraction:

GRAPES: Shower size + simulation for energy
Muon density at a given distance +simulations
Favor JACEE trends (private communication from Tonwar)

CASA/MIA: Rho(600m for muons)+ simulations
And shower size. Heavy composition favored

Hi-Res/MIA: Energy and Xmax from Hi/res (simulations needed)
Muon number from MIA (simulations)
(trend similar to JACEE?)

Next, the results from all Cherenkov experiments are presented in one slide.

Xmax from all Cherenkov Experiments: 0.5 PeV to 40 PeV

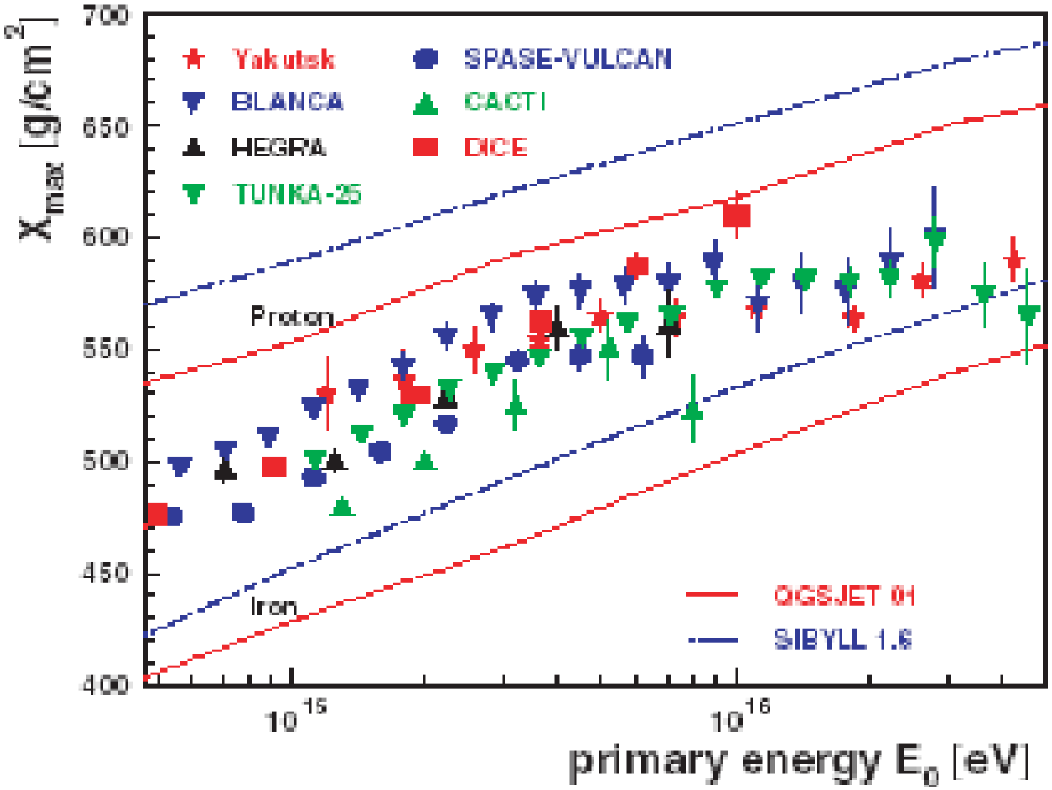

Figure 30. Compilation of different experimental results on the estimation of the shower maximum by measuring the air Cherenkov light (Yakutsk [159], BLANCA [22], HEGRA [24], TUNKA-25 [140], SPASE [48], CACTI [141], DICE [142]). Predictions by MC simulations [15] for two different models are also shown.

CACTI agrees with HEGRA AIROBIC and these two have lower Xmax with respect to DICE and BLANCA measurements below 10 PeV.

Note TUNKA has a constant Xmax above 10^16 eV .

The results from Fluorescence detector techniques are presenteed next and interpreted using fashionable models.

XMAX VERSUS ENERGY HI-RES DATA COMPARED TO ONE OF THE SIMULATIONS FOR PROTON(TOP) AND IRON(BOTTOM) .

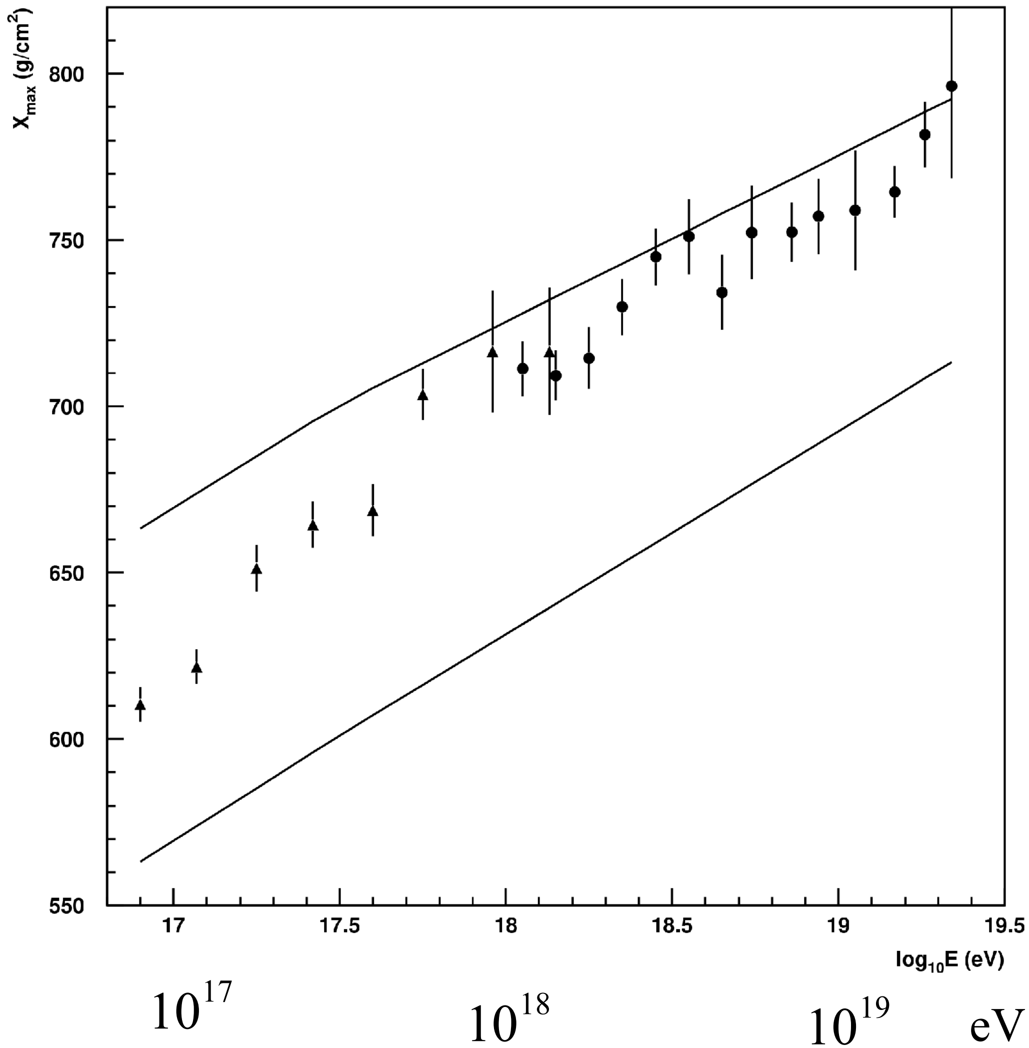

At low energies Xmax matches to that extracted by TUNKA

A compilation of all Xmax measurements compared with modelsof energy variation of shower maximum from shower simulations:

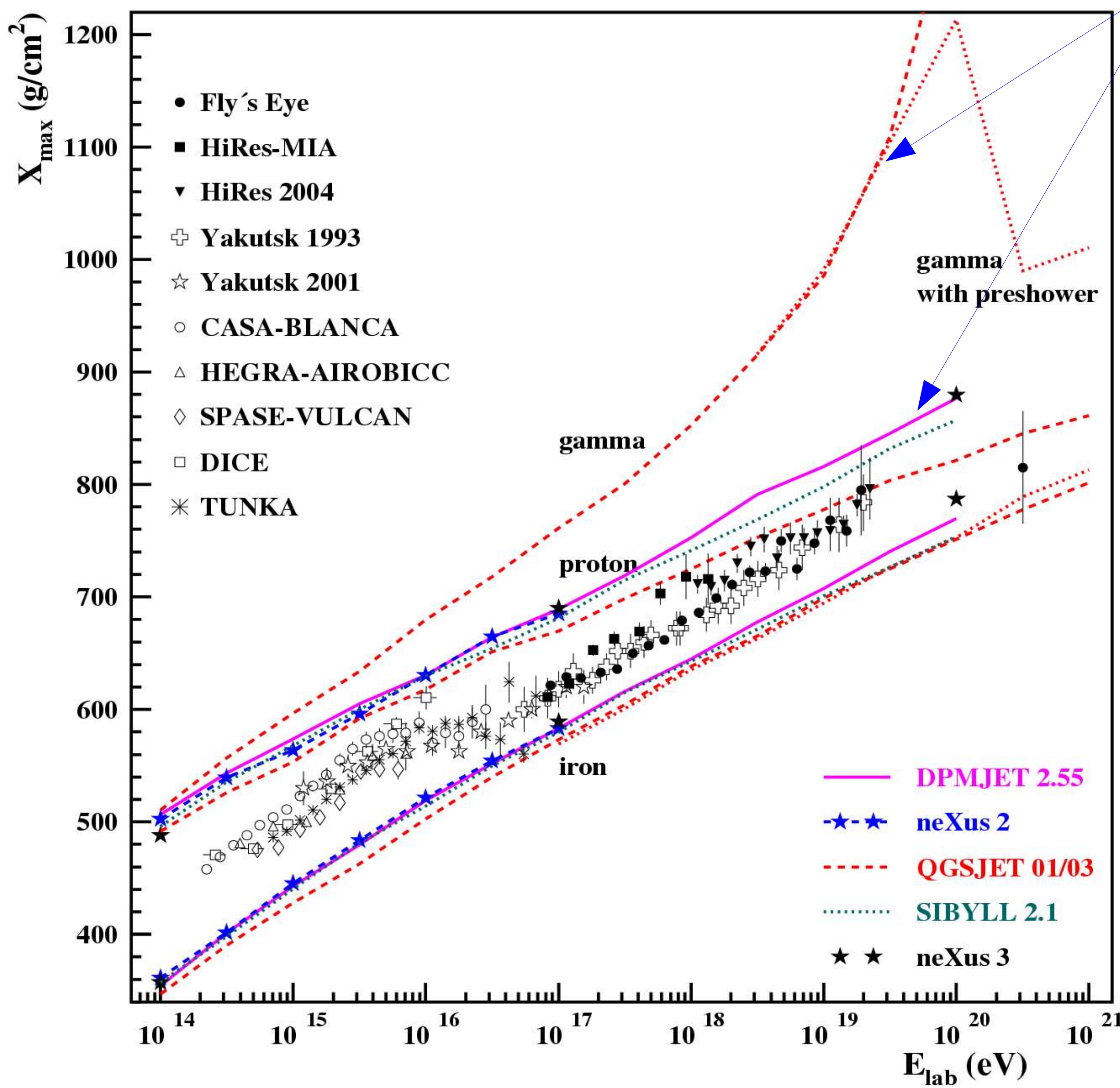

Engel 2005

Gamma and neutrino primaries can be identfied.

Composition is mixed and changing!

MC simulation (CORSIKA + Interaction Model):

Predictions depend on hadron interaction models.

Partial compensation of various effects (cross section - inelasticity)

What is the status of composition extraction from Air Shower experiments: A quick summary:

Little change since 2005.

1. Knee reflects the energy maximum of CR accelerators in the galactic sources (PWN, SNRs . . .)
2. New results from CREAM indicate agreement with previous measurements below 200 TeV . Above 200 Tev data consistent with either JACEE or RUNJOB

2. The <lnA> increases somewhere between 1 and 20 PeV

3. EGCR above the ankle – proton dominated ?

4. GCR to EGCR transition energy ? At second knee or ankle? Not resolved as yet.

General comments about extracting composition information from data:

1. Important to distinguish between measured data and extracted data that are used for confronting models to experiments.

'

2. Examples of measured data are :

ρ_{mu}, ρ_e in air showers

X_{max} in experiments which measure longitudinal profile

3. By extracted data, I mean any quantity which experimenters derrived from measured data using simulatios. Examples are:

Primary Energy E

X_{max} from Cherenkov LDF data

To improve current analyses, I strongly suggest that we carefully distinguish between measured and extracted data in doing detailed analysis to figure out whidh models best describe the data.

Extracted data need to be recomputed for each model before statistical estimation of signficance of model fits to data is attempted.

How this is best done is an open question.

My final conclusion is that our knowledge of the composition of cosmic rays and their energy spectra needs a lot more careful work before we can say that we have " determined " the composition or that we know where galactic cosmic rays end and where extra-galactic cosmic rays take over.

Current Status of models of hadronic interactions

A concern: Extraction of quantities of interest, such as Xmax, Energy, from observed AS data utilize predictions of simulations. For any quantity, not directly measured by experiment (for fluourescence method Xmax is directly measured while E is not) in principle if simulations are changed one would like to know what systematic changes arise in extracted quantities which are not directly measured.

Pierog, Engel, Heck, Ostaptchenko and Werner: 29th ECRS Sept 2006

NEW DEVELOPMENTS IN SIMULATION CODES

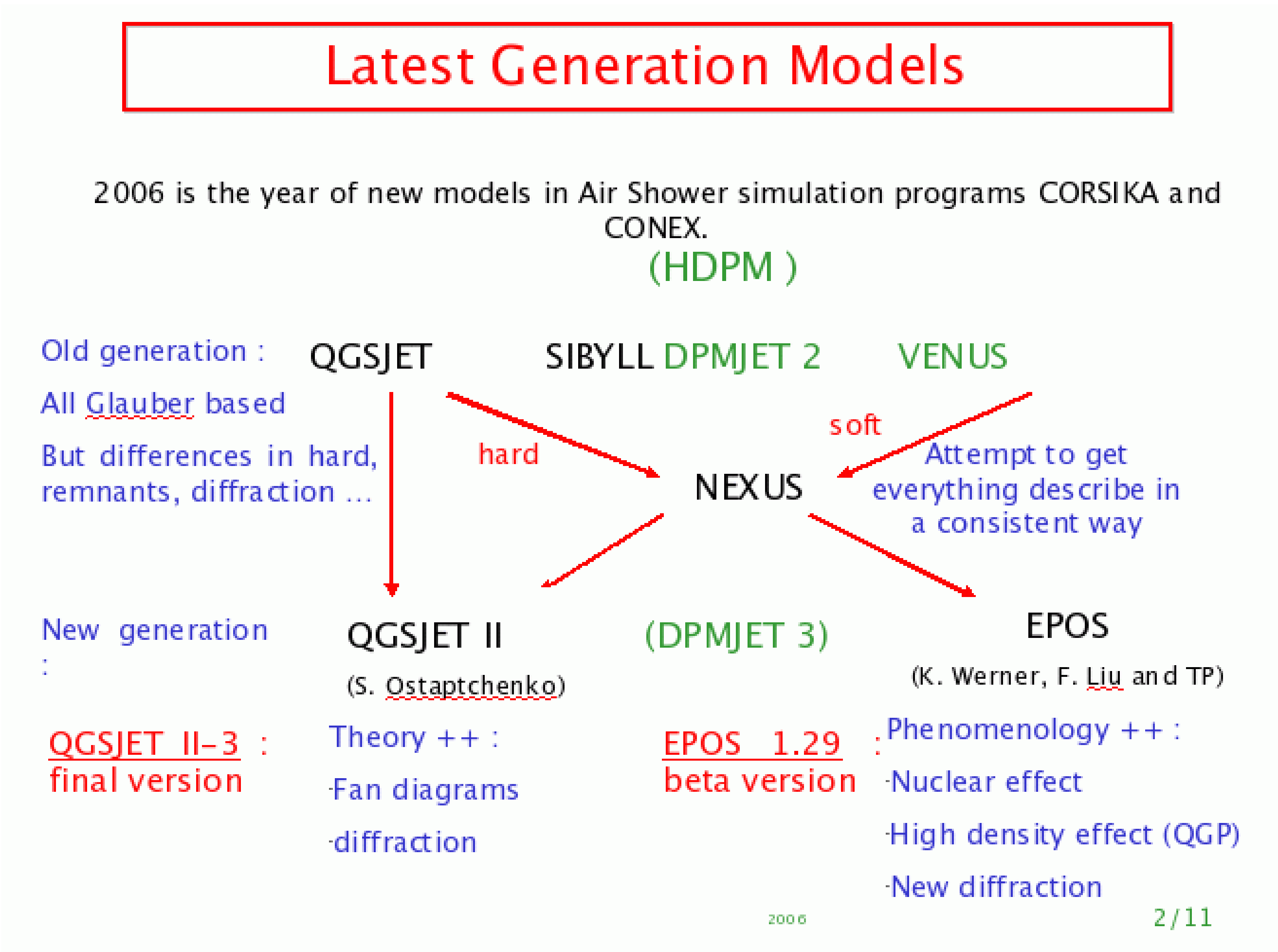

New data at low energies from NA49 data:

Note QGSJETII agrees much better with data; so does EPOS

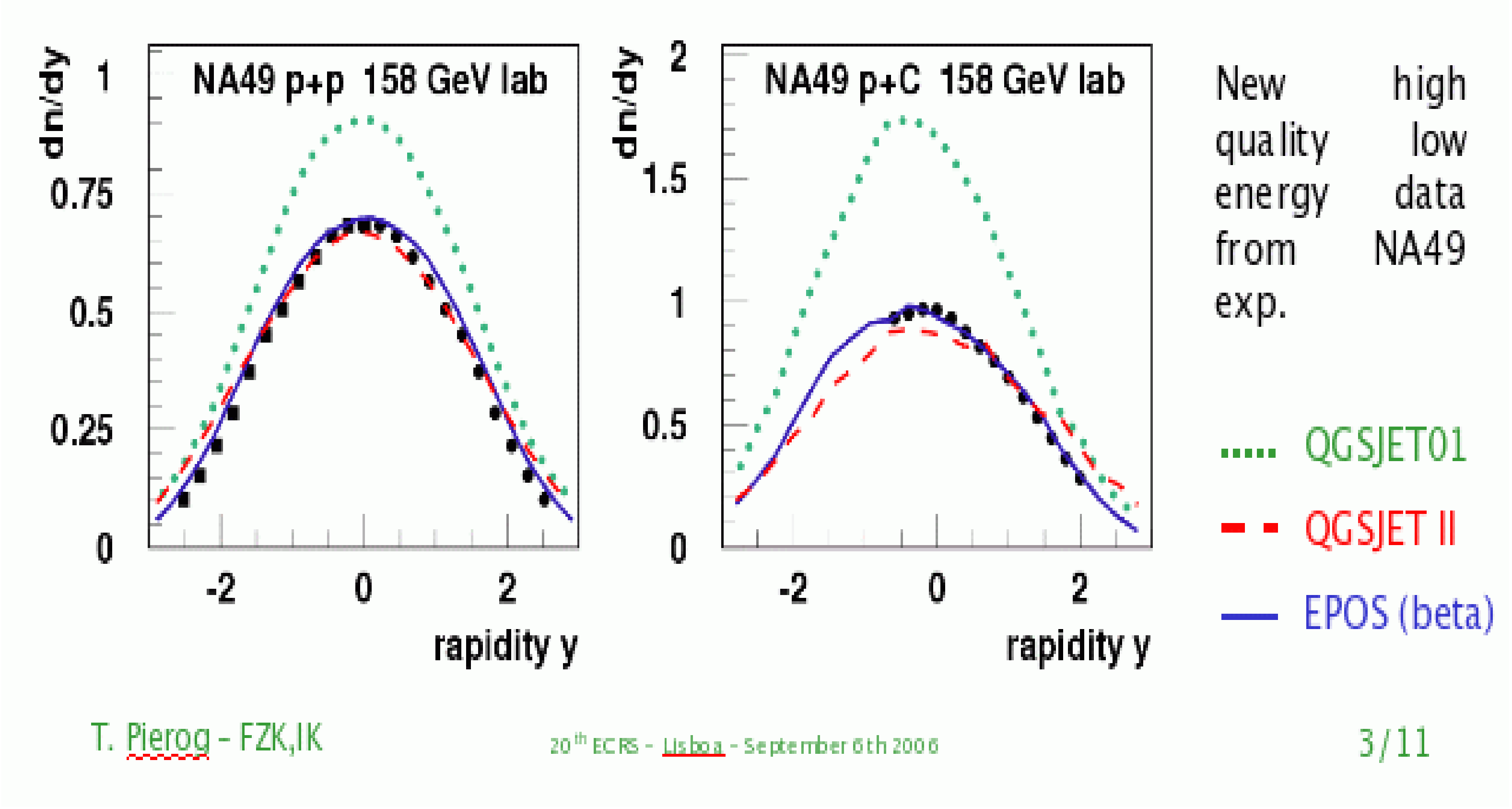

Comparision of models

p+Air Interaction

- Behavior of one of the most important interaction in Air Showers.

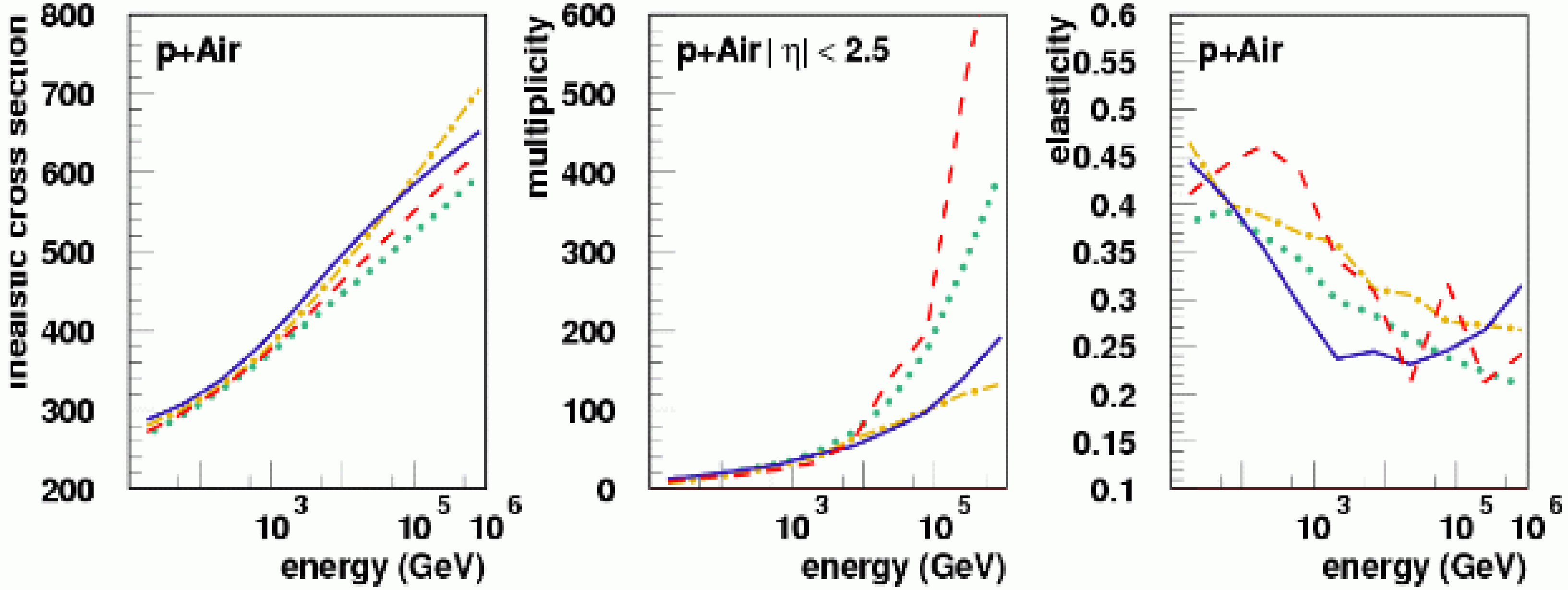

.... QGSJET01

——— EPOS (beta)

– – – QGSJET II

- · - · SIBYLL

(Low statistic for QGSJET II)

TABLE II: Average multiplicity and inelasticity per proton-proton collision.

Variable	PY 6.2	QGS 01	QGS II	SIB 2.1
p	3.8 (3.1)	3.5 (2.7)	3.9 (3.0)	2.6 (1.7)
$\overline{p}$	2.5 (3.1)	2.3 (2.2)	2.6 (2.9)	1.2 (1.6)
n	5.6 (5.9)	5.3 (5.2)	5.7 (5.7)	3.2 (3.1)
$\pi^{\pm}$	66.5 (72.1)	70.2 (68.3)	66.9 (64.5)	64.7 (60.8)
π^{0}	37.0 (40.4)	35.9 (34.9)	34.7 (33.7)	38.9 (37.2)
$K^{\pm}$	7.5 (8.9)	9.9 (9.9)	6.8 (6.9)	7.6 (8.1)
K_L	3.6 (4.5)	4.9 (5.1)	4.4 (3.7)	3.7 (4.2)
$N_{charged}$	80.3	85.9	80.3	76.1
N_{total}	126.5	139.3	136.1	125.7
$< k_L >$	0.41	0.50	0.43	0.43

Differences between models at LHC energy

Dova and Ferrari: 07

TABLE III: Most energetic secondary particle probabilities.

	Pythia 6.2	Qgsjet 01	Qgsjet II	Sibyll 2.1
proton	55.29%	43.27%	62.08%	64.62%
neutron	27.34%	18.31%	19.68%	16.51%
Σ nucleons	82.63%	61.58%	78.76%	81.13%
$\pi^{\pm}$	10.28%	20.47%	6.77%	10.72%
π^{0}	4.89%	9.74%	3.02%	5.85%
$K^{\pm}$	1.57%	2.40%	0.73%	1.00%
K_L	0.63%	0.91%	0.44%	0.57%

B. Signatures of diffractive events

For the EPOS model,the largest difference is in number of muons

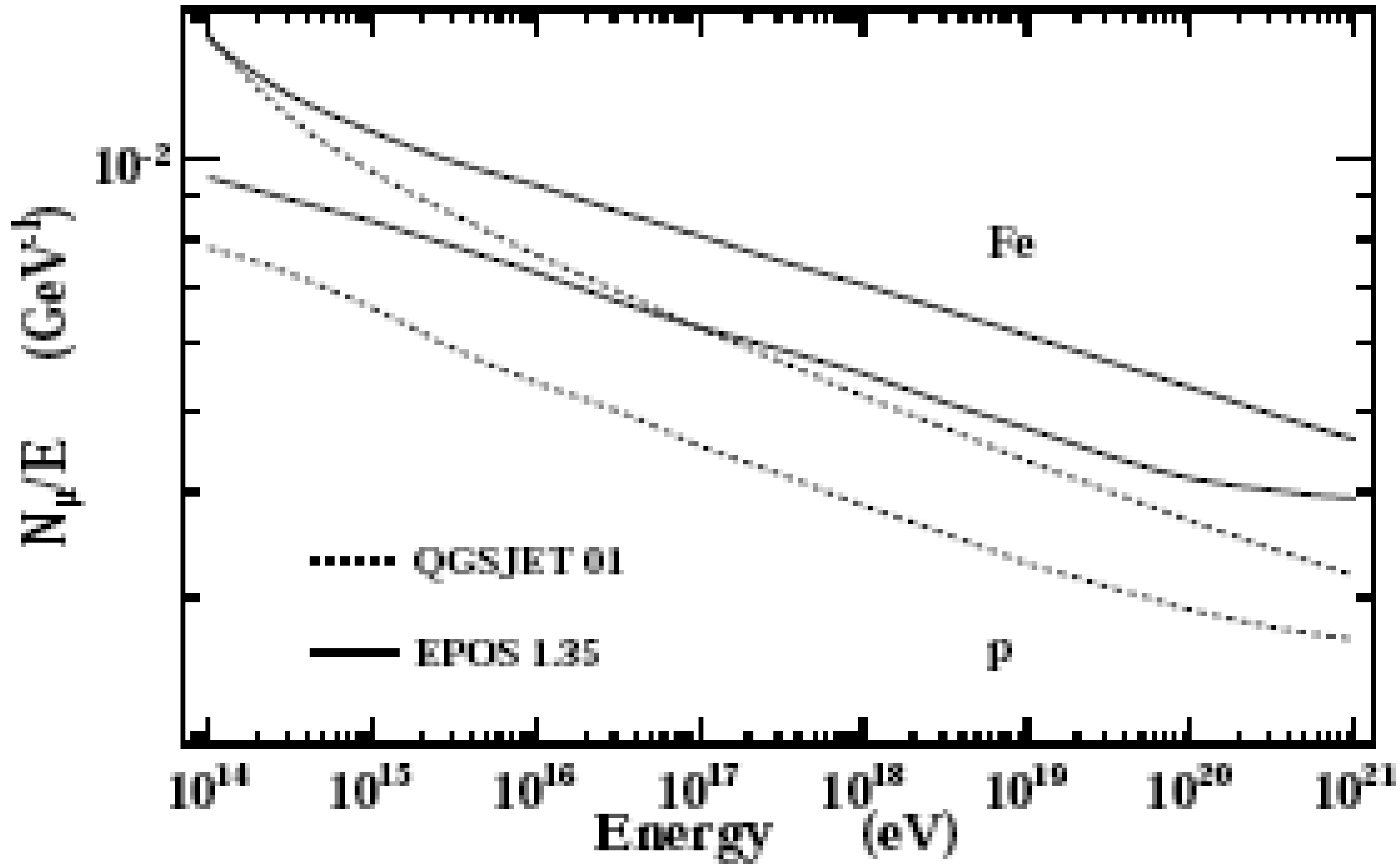

FIG. 3: Total number of muons at ground divided by the primary energy expressed in GeV as a function of the primary energy for proton and iron induced shower using QGSJET01 (dotted lines) or EPOS (full lines) as high energy interaction model.

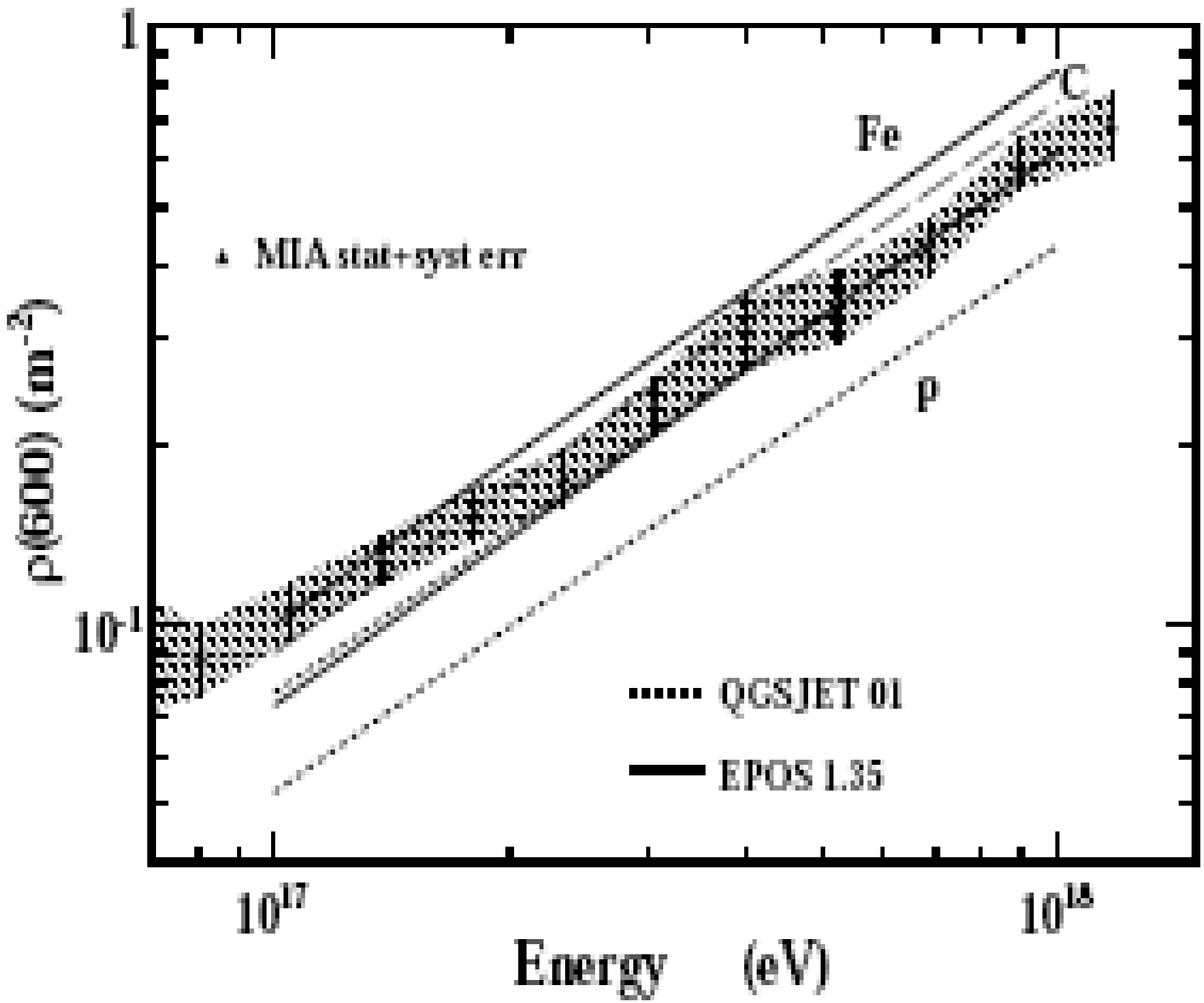

Muon density MIA experiment. Brings proton simulations closer to MIA measurements of muon density at 600 meters.

Model variations for cross section, multiplicity and its distribution and energy fraction of leading particle.

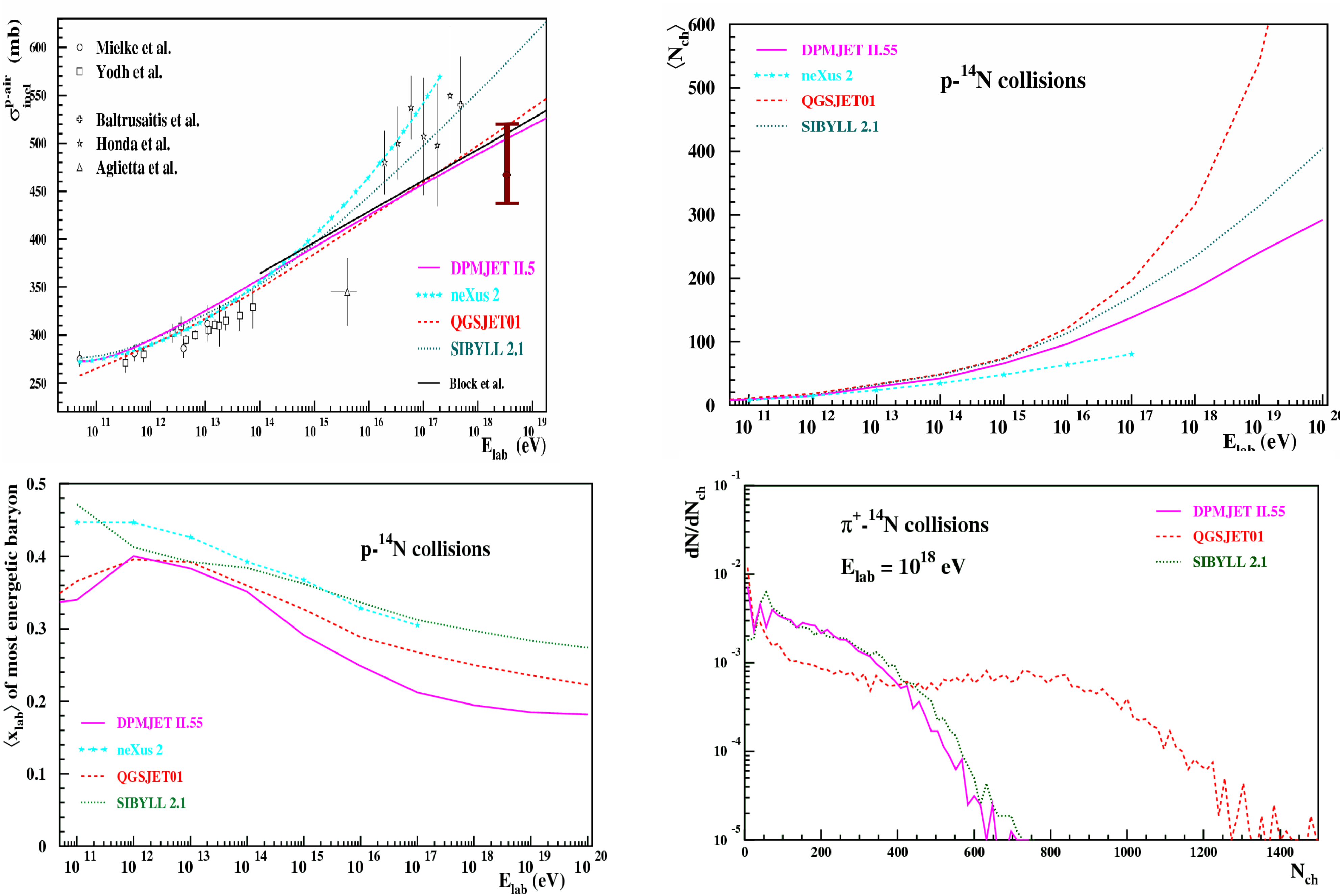

Engel 2005

Cosmic Ray Results : X_{max}

- EPOS elongation rate larger than QGSJET II one.

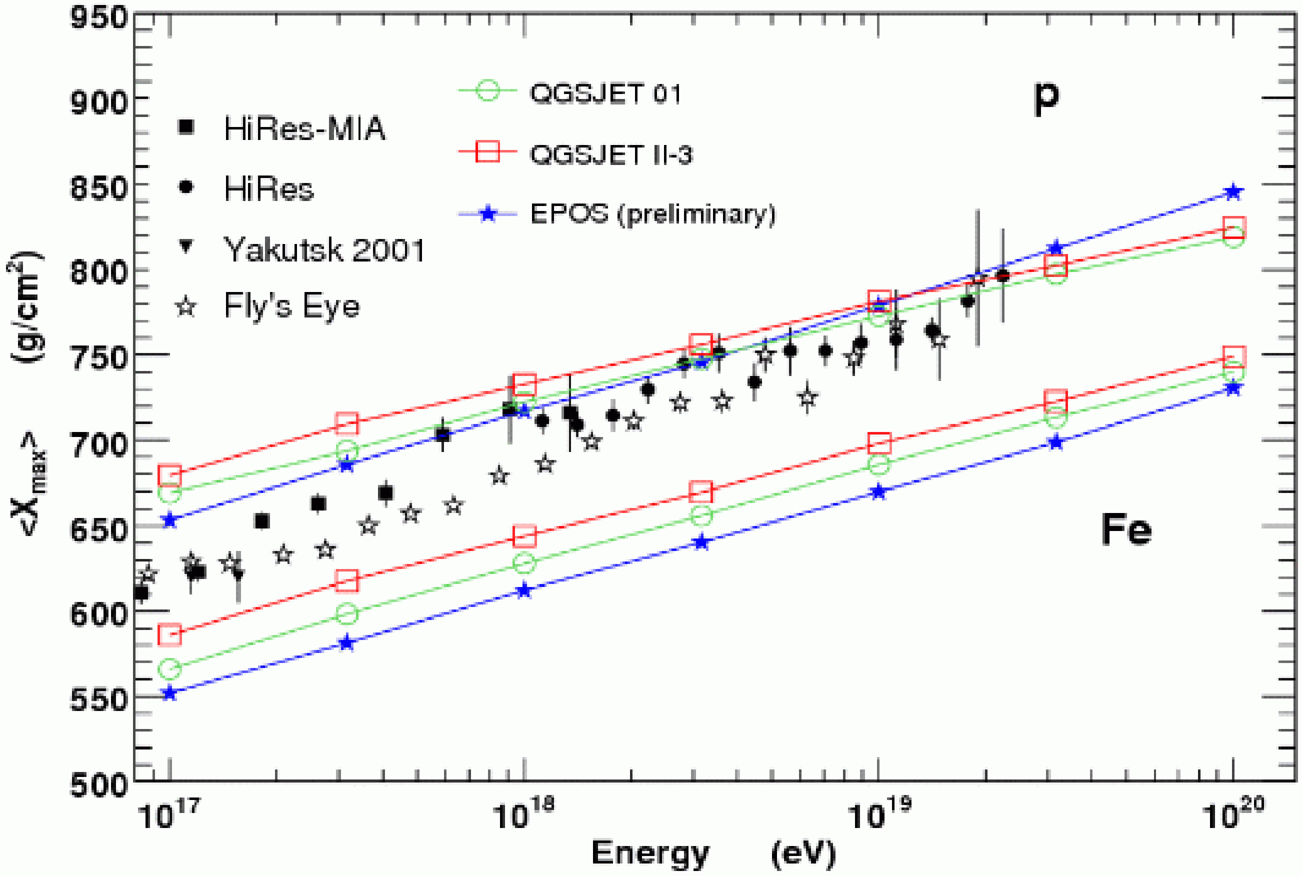

Conclusion

2 new models are now on the market (or will be soon) :

QGSJET II-3 and EPOS

- QGSJET II-3, despite more consistent extrapolation to very high energy and improvement at low energy, gives very similar results to old generation model (somewhere in between QGSJET01 and SIBYLL 2.1).
- EPOS, very preliminary results show very different results both in $<X_{max}>$ and muon number. Differences with old generation model increase with energy and seems to be more consistent with cosmic ray data.
- But now, what makes the difference in EPOS ?
  - → Sreening and nuclear effect
  - → High density effect
  - → Diffraction
  - → Bug ...
- And is it really more consistent with data ? EPOS still under development !

Concluding Remarks

Direct measurment of primary elemental composition and spectra by CREAM look very encouraging – we await results.

Measurement of Direct Cherenkov light from iron group nuclei by HESS should complement CREAM results up to about a PeV.

Measurement of coherent geosynchrotron radio emission in the low frequency regime (30-250 Mhz) by LOPES/KASKADE collaborations is a major step in improving energy measurement and directional measurement of EAS. We look forward to results from several new experiments.

The TeV gamma ray sky is ' bright ' and sample cosmic ray flux at different location in the galactic disc and neighbourhoods of many sources – SNR, PWN, etc.

The resolution of location of the end of GCR spectrum and the onset of EGCR awaits the results from AUGER and TA and TALE.